Master's Thesis

OUTAGE ANALYSIS OF LINK ADAPTATION FOR LOSSY-FORWARDING RELAYING SYSTEM

1810406 WANG YANCHEN

Supervisor	Prof. Tadashi Matsumoto
Examiners	Prof. Kurkoski Brian Michael
	Prof. Kaneko Mineo
	Prof. Amin Zribi

Graduate School of Advanced Science and Technology
Japan Advanced Institute of Science and Technology
(Information Science)

August 2020

I certify that I have prepared this Master's Thesis by myself without any inadmissible influence from outside help.

JAIST,July,2020

Author: WANG YANCHEN

(Signature)_____

Supervisor: Professor Tadashi Matsumoto

(Signature)_____

Abstract

In this thesis, we introduced a new cooperative communication strategy for single-relay Lossy Forwarding System, called Link Adaptation for Lossy-Forwarding Relaying system (LALFOR). This system aims to improve the energy efficiency and the throughput efficiency.
As many previous research has shown, the Lossy-Forwarding system can enhance the transmission reliability and expand the communication coverage. Unlike other systems, the relay of the Lossy-forwarding system will always decode, re-encode and forward the information sequences to the destination. However, since the relay will always work regardless of the channel condition, there may exist a room where the system performance can further be improved. If the channel condition is bad, relay may not be very helpful. Then always forwarding seems to cause waste of energy. On the other hand, if the channel condition is good, then keeping fixed code rate and modulation schemes will also cause the waste of throughout efficiency.
To improve the system performance, in this thesis, the LALFOR system will use two techniques, Partially-Lossy-Forwarding (PLF) technique and EXIT-based Link Adaptation Algorithm. The main idea of PLF technique is to set a threshold on the instantaneous signal-to-noise ratio of the $Source - Relay$ link. If the channel condition is bad, relay will discard the information sequences of relay. On the contrary, if the channel condition is good, relay will forward the information sequences to the destination according to the Lossy-Forwarding system. Then the energy efficiency is expected to improve by PLF although the communication coverage may decrease, then the trade-off between outage probability and communication coverage is needed. Also, since PLF will use point-to-point transmission method, it can also decrease consuming time and improve throughput efficiency. Another topic, the EXIT-based link adaptation algorithm is expected to select the code rate and modulation schemes for the $Relay-Destination$ link. The relay sends a short information sequence to acquire the quality of the $Relay - Destination$ link. Then according to the channel quality, the set of code rate and modulation scheme will be feedback from destination to relay. After that, the relay starts to forward information sequences to destination. The throughout efficiency is expected to improve by this algorithm. As the combination of PLF technique and EXIT-based Link Adaptation algorithm, LALFOR system is expected to save energy in the bad channel condition and improve the throughout efficiency whatever channel condition is.

Keywords: Lossy forwarding, Bit-Interleaving Coded Modulation with Iterative Decoding, Partially-Lossy-Forwarding, EXIT-based Link Adaptation Algorithm.

Acknowledgment

I am deeply grateful to all Matsumoto Laboratory members, Prof. Tadashi Matsumoto, Mr. Meng Cheng, Ms. Shulin Song, Mr. Lei Jiang, Mr. Wu. Li. Also, Prof. Kurkoski Brian Michael and his laboratory members helped me a lot in the two years. Especially, I received generous support from Prof. Matsumoto, who sponsored this project to let our ideas came true.
I have been in JAIST for two years. During the two years, I spent an unforgettable time with every one in our laboratory. Together, we solved the problem in the research, find new ideas, and make then come true step by step.When I was in trouble in life, they do not hesitate to give me help, which makes me moved a lot.
Thank you very much.

List of Figures

List of Tables

List of Abbreviations

AF	Amplify and Forward
AMPS	Advanced Mobile Phone System
AWGN	Additive White Gaussian Noise
BICM	Bit-Interleaved Coded Modulation
BICM-ID	Bit-Interleaving Coded Modulation with Iterative Decoding
BPSK	Binary Phase Shift Keying
CCC	Constellation Constrained Capacity
CF	Compress and Forward
CRC	Cyclic Redundancy Check
DACC	Doped Accumlator
DF	Decode and Forward
EXIT	Extrinsic Information Transfer
FER	Frame Error Rate
HI	Horizontal Iterations
LALFOR	Link Adaptation for Lossy-Forwarding Relaying system
LF	Lossy Forwarding
LLR	Log-Likelihood Ratio
MI	Mutual Information
pdf	Probability Density Function
PLF	Partially-Lossy-Forwarding
QAM	Quadrature Amplitude Modulation
QPSK	Quadrature Phase Shift Keying
SNR	Signal-to Noise Power Ratio
VI	Vertical Iterations

List of Symbols

η_{th}	Energy Efficiency
V_D	Vertical Distance
Π	a function to arrange data in non-contiguous manner to convert the bursty error to random error
E_s/N_0	the ratio of energy per symbol to the spectral noise density
E_b/N_0	the ratio of energy per bit to the spectral noise density
h	the complex fading channel gain
$p(\gamma)$	the probability density function of instantaneous SNR γ
G	the geometric gain
y	the received signal
f_c	the LLR updating function
p_e	the error probability of intra-link
$\hat{p_e}$	the assumption of error probability of intra-link
R_s	spectrum efficiency
$R_D(\cdot)$	the rate distortion function
$\mathscr{R}$	the admissible region
$H_b(\cdot)$	the function of binary entropy
$C_M(\gamma)$	the channel capacity of instantaneous SNR γ calculated by approximation function of Constellation Constrained Capacity
R_c	code rate
$\underline{M}$	the modulation method
$L(R_c, \underline{M})$	the set of signaling parameters for selected code rate and Modulation
$\gamma(L_i)$	for each set in L, the instantaneous SNR which just let the convergence tunnel open in EXIT-chart

Contents

Chapter 1

Introduction

In this chapter, we introduced the background and research motivation of Link Adaptation for Lossy-Forwarding Relaying system (LALFOR) system, then introduced the outlines and summarized the contribution.

1.1 Cooperative Wireless Communications

The main purpose of wireless communication is transmitting data efficiently and reliably. Also, improving energy efficiency and communication coverage are also the targets in the wireless communication. It is found that the above targets can be achieved by cooperative relaying system. [1] The fundamental idea of cooperative relaying system is that each relay node forward the message they received, as Fig 1.1. shows. The relays can be base stations or mobile wireless terminals. Since the relay forwarded the same information which the source transmits to the destination, the reliability of the whole system will be improved. Also the communication coverage will be improved too with the help of the relays.
Commonly, to increase the performance of cooperative wireless communication, we could set up extra relay nodes between source and the destination. Also, the outage performance will be improved by the diversity gain. Or we can allow each node to help each other with their corresponding destination [2]. Each node acts as both source and relay under different conditions.
In order to deal with different situations, relays are handled differently after receiving information. Based on the different operations , the different cooperative wireless communications systems are listed as: [3]

- Amplify and Forward (AF)
  In the AF system, the relay amplifies its received signal in any case and forwards the amplifies signal to destination. However, the relay will amplifies the error simultaneously and some practical problems will be caused due to the simple structure. [3]

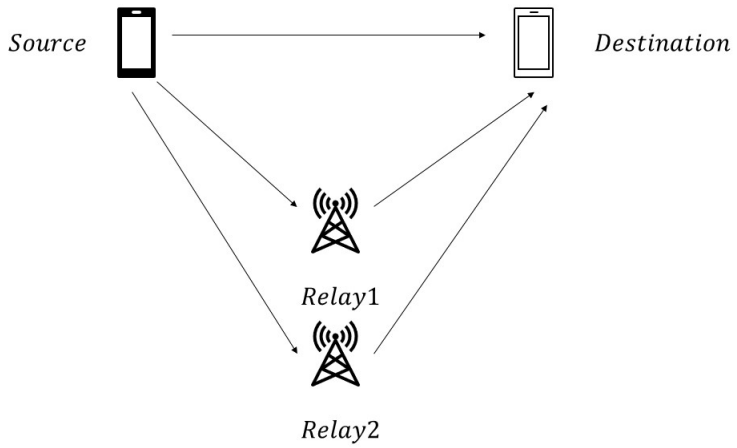

Figure 1.1: An example of cooperative wireless communication system

- Compress and Forward (CF)
  In the CF system, the relay transmits quantified and compressed information to the destination.
- Decode and Forward (DF)
  In the DF system, after receiving the signals from the source, relay firstly decode and then re-encode the information to the destination. Importantly, the relay will discard the information when decoded error has been detected. There are many practical implementations of DF protocol, such as Cyclic Redundancy Check (CRC). It is found that, DF systems outperforms AF and CF systems. However, since the relay will discard some information which still have the probabilities to decode correctly, DF system will cause a waste of the resources. Moreover, the throughout efficiency will be decreased since the error detection will be implemented at the relay. [3]

1.2 Lossy Forwarding system

To overcome the shortcomings of DF system, the Lossy forwarding system is proposed. Message will be forwarded by the relay in any case rather than discarding the information when error is detected at the relay. Better performance in outage probability could be achieved.

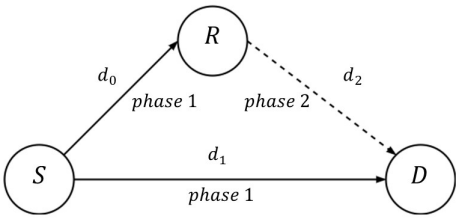

Figure 1.2: The system model of the LF system

As an example, We consider a simple three-node half-duplex relay lossy forwarding system, where a source S and a relay R and the transmission destination D, as shown in Fig1.2. In this Lossy Forwarding (LF) system, we assume a half-duplex channel which includes two phases. During the phase 1, S encodes the original message and broadcasts it to both R and D. During the phase 2,R always decodes the information even error contains in the information, re-encodes and forwards it to the destination D. After receiving signals from S and R, the joint-decoding that works on the the destination D retrieve the original message from S.

1.3 Research Motivation

The previous works in Lossy Forwarding in JAIST Information Theory and Signal Processing Laboratory is shown in Table.1.1. Although many research results about Lossy-Forwarding techniques has been found. There still exists a controversial issue which is the trade-off between coverage extension and energy efficiency loss according to the channel condition. It is mentioned by the reviewer in [9]. When the channel condition of the S-R link is bad, the relay may not offer great help to the destination. Therefore, always-forwarding strategy will cause a waste of energy. To solve this issue, this paper provide Partially-Lossy-Forwarding (PLF) technique at the relay to make a trade off between energy efficiency saving and the reduction in coverage extension according the condition of S-R link.
On the other hand, the traditional LF system utilize fixed code-rate and

Contributor	Results
Cheng et al.(2012)	Derive the theoretical outage probability over fading channels by Slepian-Wolf theorem in single-relay system. [4]
Anwar et al.(2012)	Propose an iterative decoding technique by utilizing the accumulator in turbo code for single-relay system. Also estimate and exploit the correlation between source and relay in joint decoding at destination [5]
Cheng et al.(2013)	Theoretically analyzed the outage probability of a single-relay lossy forwarding system allowing intra-link errors based on Slepian-Wolf theorem and implement BICM-ID technique in it. [6]
Zhou et al.(2014)	Obtain the calculation for exact outage probabilities in the single-relay system by utilizing the theorems for source coding with side information and Shannon's lossy source-channel separation [7]
Qian et al.(2015)	Provide an optimal power allocation scheme for a single-relay lossy forwarding system with assumed lossy transmission in source-relay link [8]
Lin et al.(2019)	Derive the admissible rate region for lossy source coding problem ,investigate the outage probability over fading channel and provide a practical encoding/decoding strategy [9]

Table 1.1: The previous work

modulation method, which may cause the waste of throughout efficiency. To improve throughout efficiency, we use Link-Adaptation technique on R-D link. The Link-Adaptation technique was a traditional method to denote the matching of the modulation, coding and other signal and protocol parameters to the conditions on the radio link in wireless communications. By using this technology on R-D link at the relay, the throughput efficiency of the relay-destination channel is expected to be improved.
By combining the PLF technique and the Link-Adaptation technique, we obtain the LALFOR system, which is expected to achieve better energy efficiency in the bad channel condition and improve throughout efficiency whatever the channel condition is.
However, whether using PLF or link adaptation technique, the outage performance will become worse. That is because in the PLF system, when the relay decide to discard the message, some message that could have been successfully decoded was discarded. And the higher code-rate and higher modulation will also decrease the outage performance. Considering the improvement of the energy efficiency and the throughout efficiency, the worse outage performance is considerable.

1.4 Summary of Contribution

This research aims to provide a new coding/decoding framework, which will save energy efficiency and throughout efficiency for the Lossy-Forwarding System. The achievement of this dissertation can be summarized as:

- We apply the PLF technique to discard messages when the channel condition of the $S - R$ link. The theoretical analysis and chain-simulation over fading channel has been implemented to calculate the increment of outage and calculated the saving energy efficiency.
- We apply the EXIT-based link adaptation algorithm technique to the $R - D$ link. Based on EXIT-analysis, an algorithm has been implemented to select the appropriate code rate and modulation.
- Finally, we combined the two systems above into LALFOR system. Then we calculate and compare the total throughput over fading channel under different conditions.

1.5 Outline of this thesis

This dissertation is organized as follows. In Chapter 1(this chapter), the research background and motivation are introduced. Then the contribution

of this research have also be summarized.
In Chapter 2, the basic knowledge of BICM-ID, joint decoding and adopted accumulator will be introduced. Also, the system model of the LALFOR system will be introduced in block diagram.
In Chapter 3, we investigate the outage analysis of the PLF system. It will include the principle of the PLF system, the definition of the energy efficiency and vertical distance. Then, the theoretical outage probability and practical Frame Error Rate (FER) comparison over fading channel, and the energy efficiency calculating under different conditions will be proposed.
In Chapter 4, We will introduce the principle of EXIT-analysis, the capacity constriction capacity. We will investigate the principle of the algorithm of the link adaptation,and show the outage probability in theoretical analysis and chain simulation.
In Chapter 5, we combined the PLF and link-adaptation as LALFOR system. The total throughput will be defined to evaluate the whole system. Benefiting from PLF and LA algorithm, the throughput efficiency is expected to improve whatever the channel condition is.
In Chapter 6, we will summarized the work in this paper and prospect the future work.

Chapter 2

Basics

In this chapter,we introduce the system model and the procedure of LALFOR System. Then the basic knowledge of Bit-Interleaving Coded Modulation with Iterative Decoding (BICM-ID) and joint decoding schemes will be introduced.

2.1 System model

2.1.1 The system model of LALFOR System

To improve the energy efficiency and the throughout efficiency, as mentioned before, we use the PLF and the EXIT-based Link adaptation technique on the original system. In phase 1, S broadcasts the original message to R and D. R decides to receive or drop based on the channel condition of the link d_0. To simplify the calculation, the condition of the link depends on the value of Signal-to Noise Power Ratio (SNR). If the SNR is lower than the setting instantaneous γ_{th}, R drop the information and only point-to-point transmission is available at this transmission. If the SNR is larger than the γ_{th}, the information will be decoded ,re-encoded and forwarded to the destination.
During phase 2 slot 1, we use the *precursor* technique to acquire the instantaneous SNR γ_2 of the link d_2. *precursor* technique is a mature technique which is invented by K. W. Cattermole in 1979 to solve pulse code modulation [10], and it is is widely used in Advanced Mobile Phone System (AMPS) in 2G times.
During phase 2 slot 2, according to the condition of $R - D$ link, the selector will choose the code rate and modulation method for next frame based on the EXIT-based Link Adaptation Algorithm.
During phase 2 slot 3, the information will be forwarded by the R to the D.

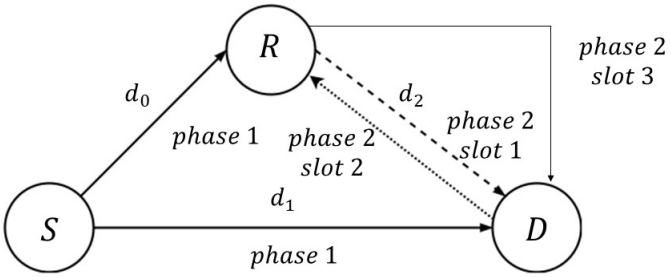

Figure 2.1: The system model of the LALFOR system

2.1.2 The decoding schemes of LALFOR System

The block diagram of LALFOR system is shown in Fig.2.2. The original message S_0 is encoded by the half-rate systematic non-recursive convolutional encoder. Then the encoded bits are doped-accumulated by a DACC. Then the outputs of the DACC are interleaved in bit order and mapped into symbols according to the specified BICM method. Then the coded information sequence is broadcast to the Relay and the Destination in phase 1. At the same time, according to the SNR of the link between Source and Relay(S-R link), relay will make a decision to keep or drop out the sequences. If the relay decides to keep the sequences, the sequences will be decoded and re-encoded. Then, to make statistically independent of S_0, the decoded message S_1 will be interleaved by an additional interleaver Π_0 Π.
During phase 2 slot 1, the relay will use *precursor* technique to acquire the SNR of the $R-D$ link.
During phase 2 slot 2, the selector will select the adaptive code rate and modulation method for S_1 according to the feedback of the channel condition of $R-D$ link based on EXIT-based Link Adaptation Algorithm.
During phase 2 slot 3, relay started sending information sequences to the destination.
After that, fully iterative decoding will be implemented horizontally and vertically at destination. During vertical iterations, the correlated error will be minimized by exploiting the correlation knowledge between the source

and the relay. Finally, after decisions of the posterior Log-Likelihood Ratio (LLR) at D_1. The recovered information sequences S_2 is obtained.

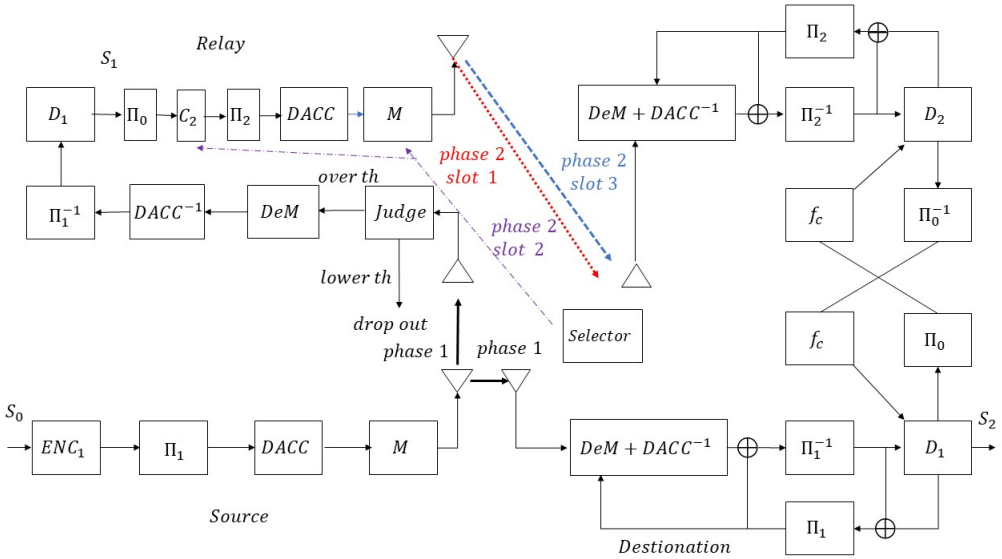

Figure 2.2: The block diagram of the LALFOR system

2.2 Channel Model

As shown in Fig 2.3., we could allocate the relay node far away from the source(Location A), near to the source(Location B), or keep the same distance to the relay and the destination(Location C). The geometric gain of the link d_2 with the regard of the link d_1 is

$$G_2 = (\frac{d_1}{d_2})^{\alpha}, \tag{2.1}$$

where α is the path-loss which is assumed to be 3.52 [11]. Also the geometric gain of the link d_0 with the regard of the link d_1 is

$$G_0 = (\frac{d_1}{d_0})^{\alpha}. \tag{2.2}$$

Moreover, since the generality is lossless in link d_1, the geometric gain G_1 is fixed as one. Then the received signals $y_i (i = 0, 1, 2)$ are

$$y_1 = \sqrt{G_1} \cdot h_1 \cdot t_1 + n_1, \tag{2.3}$$
$$y_2 = \sqrt{G_2} \cdot h_2 \cdot t_2 + n_2, \tag{2.4}$$
$$y_3 = \sqrt{G_3} \cdot h_3 \cdot t_3 + n_3, \tag{2.5}$$

where n_i denoted the Additive White Gaussian Noise (AWGN) noise vector which the mean is 0 and the variance is σ_n^2 in each dimension. h_i denotes the complex fading channel gain, specifically, the normalized variance $\langle |h_i|^2 \rangle$ is 1 when the link suffers from white Gaussian noise. h_i will change variously under fading channel. t_1 and t_2 represent the message vector transmitted transmitted from source and relay. Given the path-loss exponent is 3.52, we can found at Location A

$$\Gamma_0 = \Gamma_1 + 14.0075[dB],$$
$$\Gamma_2 = \Gamma_1 + 7.8094[dB],$$

and Location B

$$\Gamma_2 = \Gamma_1 + 14.0075[dB],$$
$$\Gamma_0 = \Gamma_1 + 7.8094[dB]. \tag{2.6}$$

Also, we assume each link suffer from block-fading, the instantaneous SNR of d_1 is expressed as

$$\gamma_1 = \frac{G_1 |h_1|^2 E_s}{N_0}, \tag{2.7}$$

and with the assumption $\langle |h_i|^2 \rangle = 1$, the average SNR is

$$\Gamma_1 = \frac{G_1 E_s}{N_0}, \tag{2.8}$$

where spectral noise power density in both-dimension N_0 is defined as $N_0 = 2\sigma_i^2 \, (i = 0, 1, 2)$ without loss of generality. Same equation can be expressed in d_0 and d_2. Then the Probability Density Function (pdf) of γ_i is expressed as: [12]

$$p(\gamma_i) = \frac{1}{\Gamma_i} \exp(-\frac{\gamma_i}{\Gamma_i}). \quad i = 0, 1, 2. \tag{2.9}$$

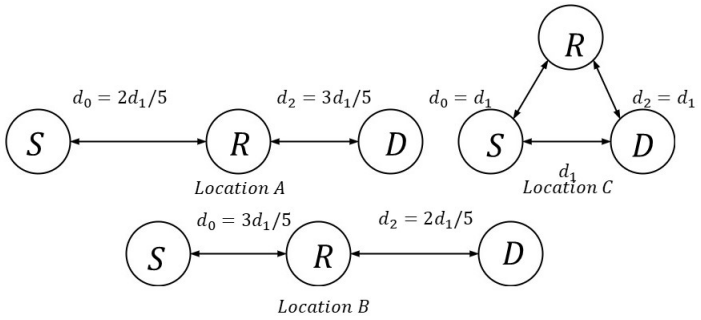

Figure 2.3: The system model of the different relay location

2.3 Doped Accumulator

The Doped Accumlator (DACC) is a technique which is utilized to achieve better performance. In Extrinsic Information Transfer (EXIT) analysis, it was found [13] by using this technique, the inner code EXIT curve can be pushed up and reach the (1,1) Mutual Information (MI) point.
The structure of the doped accumulator is same as the memory-1 half rate systematic recursive convolutional code in Fig 2.7. The process of doped accumulator is expressed as

$$b(k) = \begin{cases} s_k, if\ k\ mod\ P_d \neq 0 \\ b_{k-1} \oplus s_k, if\ k\ mod\ P_d = 0, \end{cases} \tag{2.10}$$

where P_d is the doping ratio of the selector, it means every P_d bit the ACC outputs the accumulated bits. b_k denotes the bits which is accumulated and the b_k is same as input a_k. Specifically, b_k is set as 0 at the beginning.
As an example in Fig.2.4, the input sequence is $\{s_1, s_2, s_3, s_4, s_5, s_6, s_7, s_8\}$ and the outputs of the accumulator is$\{b_1, b_2, b_3, b_4, b_5, b_6, b_7, b_8\}$ and the doping ratio P_d is 2. Therefore the result will be $\{s_1, b_2, s_3, b_4, s_5, b_6, s_7, b_8\}$

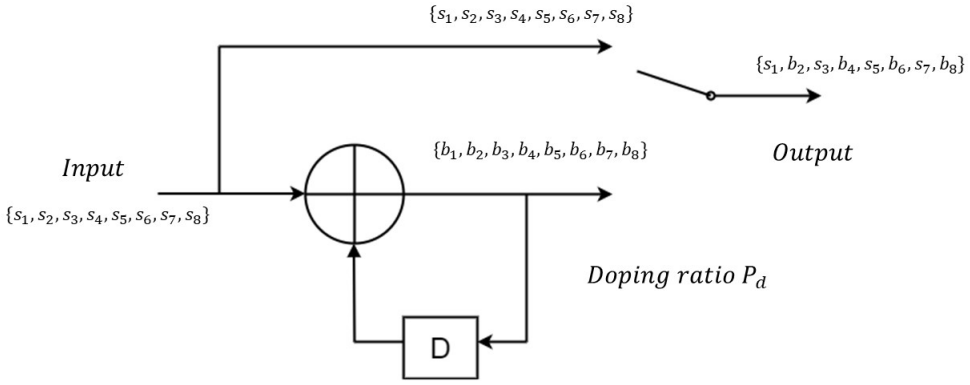

Figure 2.4: The system model of Doped Accumulator

2.4 Bit-Interleaved Coded Modulation with Iterative Decoding(BICM-ID)

Bit-Interleaved Coded Modulation (BICM) was proposed by Zehavi [14]. It is considered as an efficient transmission over Rayleigh fading channels. [15] As shown in Fig 2.5., each bit of the coded code from the convolutional encoder is interleaved by the bit interleaver and then mapped on to a symbol with a specified mapping rule. The interleaver will diffuse the busty errors caused by the correlated fading in the channel and distributing the bits to make them independent with each other. [16] The BICM techniques increase the independence of the information from bit level to symbol level.

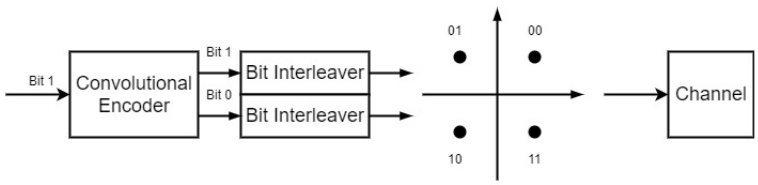

Figure 2.5: The BICM transmitter model in QPSK

Also, the specified mapping rule which BICM use, which is called non-Gray mapping rule, could obtain more knowledge from the demapper in each

iteration and achieve better performance finally. To explain the mechanism of the non-Gray mapping rule, we offer an example as Fig 2.6. We assume in the QPSK demapping procedure, we can obtain the full prior information for Bit A. Hence, the pattern for Bit B can be detected by comparing the Euclidean distance which is shown in Fig 2.6. Obviously, non-Gray mapping has longer Euclidean distance than Gray Mapping. Therefore, the non-Gray mapping pattern could achieve better performance than the Gray-mapping. At the receiver side, BICM-ID was originally published in [17], by Li and Ritcey. The output of the demapper is the *extrinsic* LLR L_E as [18], which is based on maximum aposterior probability(MAP) algorithm

$$\begin{aligned} L_E(s_v) &= ln\frac{P_r(s_v=1|y)}{P_r(s_v=0|y)} \\ &= ln\frac{\sum_{s\in S_1}\left\{\exp\left\{-\frac{|y-s|^2}{2\sigma_n^2}\right\}\prod_{w\neq v}^{N}\exp(s_w L_a(s_w))\right\}}{\sum_{s\in S_0}\left\{\exp\left\{-\frac{|y-s|^2}{2\sigma_n^2}\right\}\prod_{w\neq v}^{N}\exp(s_w L_a(s_w))\right\}}, \end{aligned} \tag{2.11}$$

where N presents the length of the symbol and $L_a(s_w)$ represents the prior information $L^c_{a',D}$,which is the interleaved at the *w-th* position in a symbol, and S_1 denotes the mapping pattern of the *v-th* bits in a symbol.
As shown in Fig.2.7, after the process of $DACC^{-1}$ at the S-D link, the *extrinsic* LLR $L^c_{e',D1}$ is de-interleaved by the Π_1^{-1}.Then, the *extrinsic* LLR $L^c_{e',D1}$ is changed to the *priori* LLR $L^c_{a,D1}$ for decoder D_1. The output of decoderD_1 contains the posterior LLR $L^c_{p,D1}$ for coded bits, and posterior LLR $L^u_{p,D1}$ for systematic bits. Then we subtract the *priori* LLR $L^c_{a,D1}$ from posterior LLR $L^c_{p,D1}$ to obtain the new *extrinsic* LLR $L^c_{e',D1}$. After interleaver, the new *priori* LLR $L^c_{a',D1}$ is feedback to the $Demapper + DACC^{-1}$. The process of the Horizontal Iterations (HI) can be expressed as:

$$L^c_{e,D1} = L^c_{p',D1} - L^c_{a',D1}, \tag{2.12}$$
$$L^c_{a,D1} = \Pi_1^{-1}(L^c_{e,D1}), \tag{2.13}$$
$$L^c_{e',D1} = L^u_{p,D1} - L^c_{a,D1}, \tag{2.14}$$
$$L^c_{a',D1} = \Pi_1(L^c_{e',D1}) \tag{2.15}$$

This horizontal iterative loop will be finished by specified times or no more posterior information can be founded. Then the obtained posterior LLR $L^u_{p,D1}$ is put into the Vertical Iterations (VI).

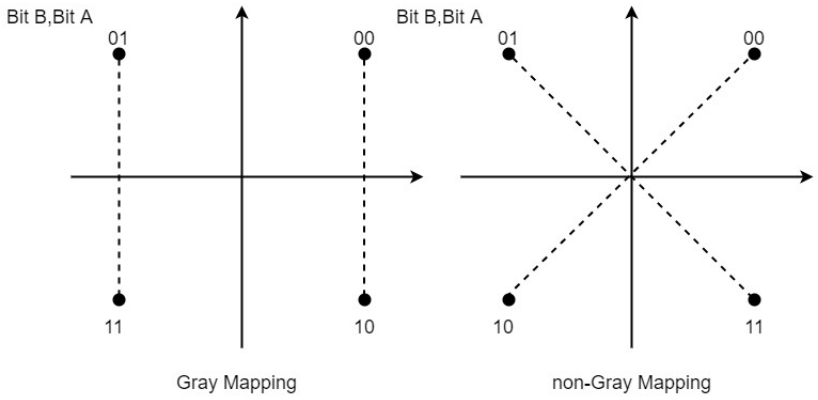

Figure 2.6: Mapping rules for Gray and non-Gray in QPSK

2.5 Joint decoding and LLR Updating Function

As shown in Fig 2.8, now we focused on the vertical iterations after the horizontal iterations are finished. By utilizing the correlation knowledge between the source and relay, we can minimize the correlated error in vertical iterations. The correlation value is denoted by the error probability p_e of the intra-link. It can be estimated by the posterior LLRs of the uncoded(systematic) bits, which are $L^u_{p,D1}$ and $L^u_{p,D2}$. $L^u_{p,D1}$ and $L^u_{p,D2}$ are obtained from the decoders *D1* and *D2*, and p_e is calculated by

$$\hat{p_e} = \frac{1}{N}\sum_{n=1}^{N}\frac{\exp(L^u_{p,D1}) + \exp(L^u_{p,D2})}{(1+\exp(L^u_{p,D1}))(1+\exp(L^u_{p,D2}))}, \tag{2.16}$$

where N represents the number of the posterior LLR pairs from the decoders $D1$ and $D2$.
Then we can calculate the probability of the data sequences u_s and u_r as

$$Pr(u_{s,n}=0) = (1-\hat{p_e})\cdot Pr(u_{r,n}=0) + \hat{p_e}\cdot Pr(u_{r,n}=1) \tag{2.17}$$
$$Pr(u_{s,n}=1) = (1-\hat{p_e})\cdot Pr(u_{r,n}=1) + \hat{p_e}\cdot Pr(u_{r,n}=0), \tag{2.18}$$

where u_s and u_r denotes the information from source and relay and $u_{s,n}$ and $u_{r,n}$ denotes the t-th elements of u_s and u_r.From [19] we know the LLR updating function for u_s is

$$L(u_{s,t}) = ln\frac{Pr(u_{s,t}=0)}{Pr(u_{s,t}=1)} = ln\frac{(1-\hat{p_e})\cdot\exp[L(u_{r,t})] + \hat{p_e}}{(1-\hat{p_e}) + \hat{p_e}\cdot\exp[L(u_{s,t})]}, \tag{2.19}$$

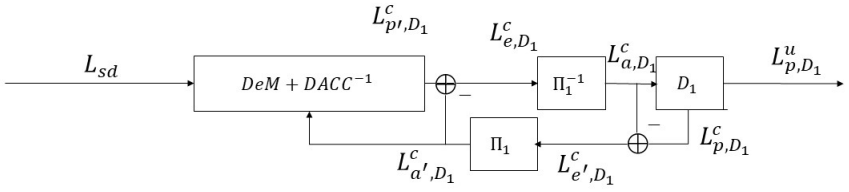

Figure 2.7: The system model of BICM-ID in the horizontal iterations

and for u_r is

$$L(u_{r,t}) = ln\frac{Pr(u_{r,t}=0)}{Pr(u_{r,t}=1)} = ln\frac{(1-\hat{p_e})\cdot\exp[L(u_{r,t})]+\hat{p_e}}{(1-\hat{p_e})+\hat{p_e}\cdot\exp[L(u_{r,t})]}, \tag{2.20}$$

Generally, the LLR updating function f_c is given as

$$f_c(x,\hat{p_e}) = ln\frac{(1-\hat{p_e})\cdot\exp(x)+\hat{p_e}}{(1-\hat{p_e})+\hat{p_e}\cdot\exp(x)}, \tag{2.21}$$

where x denotes the input value of *extrinsic* LLRs $L^u_{e,D1}$ and $L^u_{u,D2}$. They are obtained by subtracting the uncoded *priori* LLR $L^u_{a,D}$ from the uncoded posterior LLR $L^u_{p,D}$.The VI can be expressed as

$$L^u_{a,D1} = f_c(\Pi_0^{-1}(L^u_{e,D2})), \tag{2.22}$$

$$L^u_{a,D2} = f_c(\Pi_0(L^u_{e,D1})). \tag{2.23}$$

After the iterations in the horizontal iterations and vertical iterations, the final judgement is according to the uncoded LLR $L^u_{p,D1}$.

2.6 Summary of this Chapter

In this chapter, we introduced the system model of LALFOR System firstly. Then, we introduced the principle of the DACC, the basic knowledge of the decoding schemes. It contains two main parts, BICM-ID in the horizontal decoding iterations, and LLR updating in vertical iterations.

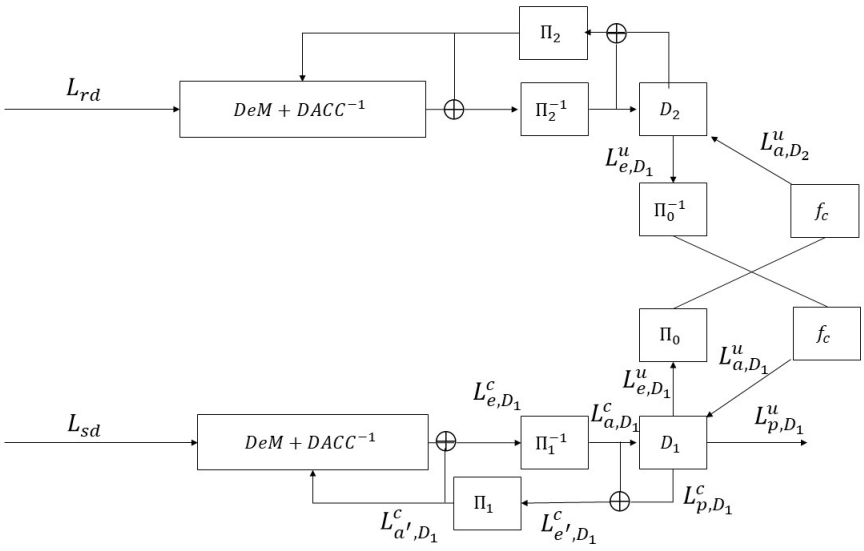

Figure 2.8: The system model of joint decoding and LLR updating

Chapter 3

Partially Lossy Forwarding System

In this chapter, we apply the PLF technique to the single-relay Lossy Forwarding system. We will display the system model of PLF firstly, then show the process of exact outage probability analysis. Finally, the theoretical and chain-simulation results will be presented.

3.1 System Model

We consider a single relay system, as shown in Fig.3.1. We assume all the links are under block-fading and the instantaneous SNR of $S-R$ link is γ_0 and the instantaneous SNR of setting threshold is γ_{th}. If the γ_0 is larger than γ_{th}, the Source will broadcast the information sequences to the Relay and Destination. Then, the Relay decoded the information sequence,de-interleaves and interleaves the information, re-encoded it and forwarded to the Destination. If the γ_0 is smaller than γ_{th}, the Relay will discard the information sequences, then only $S-D$ link is available.
The purpose of PLF technique, is to improve energy efficiency in the bad channel condition. However, the outage performance of PLF will become worse than the traditional Lossy Forwarding System(LF System) because the decoder at the destination can not receive the help from the relay when the γ_0 is lower than γ_{th}. Therefore, we must carefully choose γ_{th} to make a good trade off between communication coverage and energy efficiency.

3.2 Intra-Link error probability analysis

In this section, we will identify the relationship between the intra-link probability p, the instantaneous SNR γ_0 and the setting threshold γ_{th}. According to Shannon's lossy source-channel separation theorem [12].

$$R_s \cdot R(D) \leq C(\gamma), \tag{3.1}$$

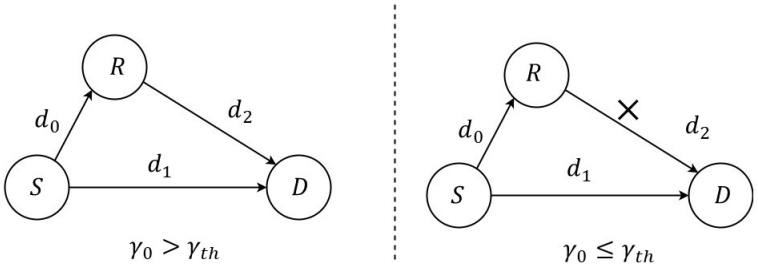

Figure 3.1: The system model of PLF System

where R_{s0} denotes the spectrum efficiency of the intra-link d_0, and $R(D)$ is the rate-distortion function of the source. $C(\gamma_0)$ denotes the channel capacity of the intra-link d_0. With Hamming distortion measure, the distortion level D is equal to the intra-link probability p. By substituting p into (3.1) we can obtain $R(p) = \Phi_1(\gamma_0) = \frac{C(\gamma_0)}{R_{s0}}$. Let $H_b(x)$ denotes the function of the binary entropy, which is $H_b(x) = -x \cdot log_2(x) - (1-x)log_2(1-x)$. $H_b^{-1}(x)$ denotes the inverse function of the $H_b(x)$, we can express p as:

$$p = \begin{cases} H_b^{-1}[1 - \Phi_1(\gamma_0)], & \text{for } \Phi_0^{-1}(0) \leq \gamma_0 \leq \Phi_0^{-1}(1) \\ 0, & \text{for } \gamma_0 \geq \Phi_0^{-1}(1) \end{cases} \tag{3.2}$$

Therefore, it is obvious to find out the relationship between the average SNR of $S - R$ link to p as shown in Fig.3.2. Also, from (3.2), we can find the relationship between setting threshold γ_{th} and intra-link error probability p_{th} as:

$$p_{th} = H_b^{-1}[1 - \Phi_1(\gamma_{th})]. \tag{3.3}$$

Also, according to Shannon's separation theorem, for Source-Destination link and Relay-Destination link, if the transmission rates and spectrum efficiency $R_{s,1}$ and $R_{s,2}$ satisfy:

$$\begin{cases} R_1 R_{s,1} \leq C(\gamma_1) \\ R_2 R_{s,2} \leq C(\gamma_2). \end{cases} \tag{3.4}$$

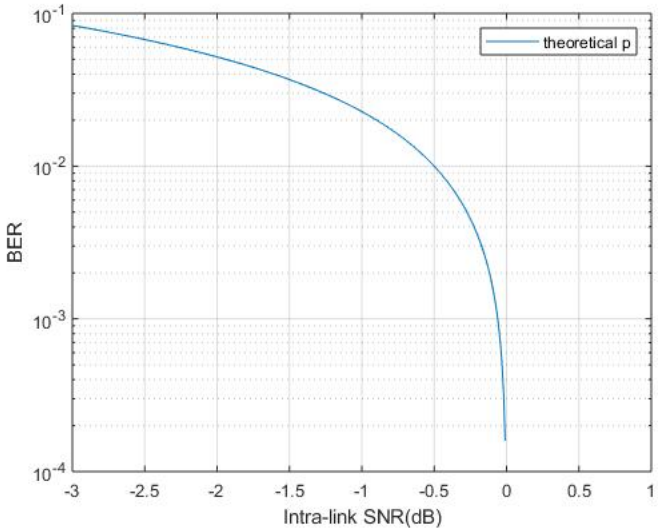

Figure 3.2: Theoretical BER of intra-link with rate distortion function

The error probability can be arbitrarily small, where $C(\gamma_1)$ and $C(\gamma_2)$ denotes the throughout efficiency of Source-Destination link and Relay-Destination link with the instantaneous SNR γ_1 and γ_2.
Then the relationship between rate R_1 and R_2 and the instantaneous SNR γ_i is

$$R_1 = \Phi_1(\gamma_1) = \frac{C(\gamma_1)}{R_{s1}} \tag{3.5}$$

$$R_2 = \Phi_2(\gamma_2) = \frac{C(\gamma_2)}{R_{s2}}, \tag{3.6}$$

and for their inverse function:

$$\gamma_1 = \Phi_1^{-1}(R_1) = C^{-1}(R_1, R_{s1}) \tag{3.7}$$

$$\gamma_2 = \Phi_2^{-1}(R_2) = C^{-1}(R_2, R_{s2}), \tag{3.8}$$

where $C^{-1}(R_i, R_{si})$ represents the inverse function of channel capacity. and $C^{-1}(R_i, R_{si})$

3.3 Exact outage probability analysis

3.3.1 Theoretical Analysis

As shown in Fig. 3.3. We considered U_1 as the ordinary binary information sequence,U_2 as the output of the encoder of Source. As written in the previous

section, U_2 can be seen as the result of bit-flipped of U_1, with probability p, which can be expressed as:

$$U_2 = U_1 \oplus P \, mod \, 2, \tag{3.9}$$

where $\Pr(P = 1) = 1 - \Pr(P = 0) = p$.
Also, $\hat{U_1}$ is the output of the decoder at the destination and $\hat{U_2}$ is the estimate of U_2. Let R_1 and R_2 be the rates of Source-Destination link($S - Dlink$) and Relay-Destination link($R - Dlink$). Since the information from source to destination and from relay to destination are correlated, and the information from relay help the destination recover the information from the source, we can use the theorem for source coding with side information to find the requirement which $\hat{U_0}$ is a successful recovery of U_0, which is :

$$\begin{cases} R_1 \geq H(U_1|\hat{U_2}) \\ R_2 \geq I(U_2; \hat{U_2}), \end{cases} \tag{3.10}$$

$H(U_1|\hat{U_2})$ is conditional entropy of $H(U_1)$, and the $I(U_2; \hat{U_2})$ is the mutual information between $H(U_1)$ and $H(\hat{U_2})$. We assume the relationship between $\hat{U_2}$ and U_2 is the bit-flipping with probability $p^{'}$, obviously $H(U_1|\hat{U_2}) = H_b(p^{'} * p)$, where $p^{'} * p = (1 - p^{'})p + (1 - p)p^{'}$. Also $I(U_2; \hat{U_2}) = H(\hat{U_2}) - H(\hat{U_2}|U_2) = 1 - H_b(p^{'})$

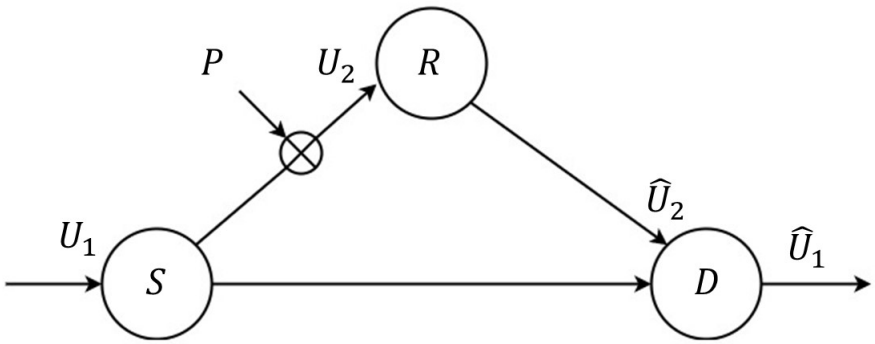

Figure 3.3: The system model of coding and decoding with side information

3.3.2 Exact Outage Probability when $\gamma_0 > \gamma_{th}$

As shown in Fig.3.4., we can divided the rate-region into 3 sub regions:Region $\mathscr{R}_A$,Region $\mathscr{R}_B$,Region $\mathscr{R}_C$.Region $\mathscr{R}_A$ denotes the case when outage event happens if the $R_2 \geq 1$, which means the information are successfully decoded at the relay. Region $\mathscr{R}_B$ denotes the case when outage event happens if the $R_2 \leq 1$, which means the information decoded at the relay contains error. Region $\mathscr{R}_C$ denotes the case when outage event did not happen, which means admissibly region.
Therefore, when $\gamma_0 > \gamma_{th}$, which means relay is always working, the probability for (R_1, R_2) fall in $\mathscr{R}_A$ and $\mathscr{R}_B$, which is equal to the outage probability, can be expressed as:

$$\begin{aligned} P_{out}^{C_1} &= \Pr(0 \leq p < p_{th}, (R_1, R_2) \epsilon (R_A \cup R_B)) \\ &= \Pr(p = 0, (R_1, R_2) \epsilon R_A) \\ &+ \Pr(p = 0, (R_1, R_2) \epsilon R_B) \\ &+ \Pr(0 < p < p_{th}, (R_1, R_2) \epsilon R_A) \\ &+ \Pr(0 < p < p_{th}, (R_1, R_2) \epsilon R_B), \end{aligned} \tag{3.11}$$

When $R_2 \geq 1$, to reach $\mathscr{R}_C$, R_1 should larger than $H_b(0 * p) = H_b(p)$. When $R_2 \leq 1$, to reach $\mathscr{R}_C$, R_1 should larger than $H_b(p^{'} * p)$. Generally, R_1 should satisfies (3.12) to reach admissible region:

$$R_1 \geq \begin{cases} H_b(p), & for\, R_2 \geq 1, \\ H_b(p^{'} * p), & for\, 0 \leq R_2 \leq 1, \end{cases} \tag{3.12}$$

3.3.3 Exact Outage Probability when $\gamma_0 \leq \gamma_{th}$

Obviously, since relay will discard the information sequence when $\gamma_0 \leq \gamma_{th}$, only point-to-point transmission is available under this condition. Successful decoding of U_1 satisfies $R_1 \geq H(U_1)$, which is equal to $R_1 \geq H(p)$. So the outage probability can be expressed as

$$P_{out}^{C_2} = \Pr(p_{th} \leq p \leq 0.5, 0 \leq R_1 \leq H_b(p)). \tag{3.13}$$

3.4 The definition of Energy Efficiency and Vertical Distance

Before we process the theoretical simulations, we need to make a clear definition of the energy efficiency η_{th} and the vertical distance from relay

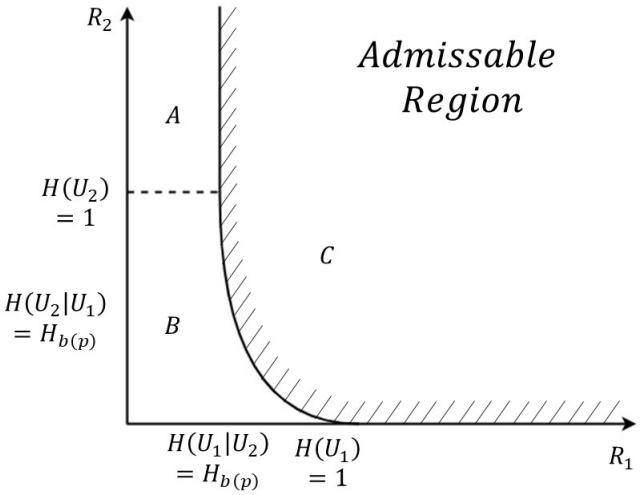

Figure 3.4: The admissable rate region by the theorem for source coding with side information

to S-D link V_D.
The energy efficiency (th) is defined as the ratio of bits discarded by relay nodes to total transmission bits under γ_{th}, which is expressed as:

$$\eta_{th} = \frac{N_{th}}{N_{all}}. \tag{3.14}$$

As shown in Fig. 2.3. In the tradition Lossy-Forwarding system, we assume the relay moves on the line between the source node and the end point. However, this assumption will cause geometric loss. To compensate it, we introduce the vertical distance V_D in the PLF system. The vertical distance is defined as the ratio of the vertical distance d_{st} from relay to S-D link to the distance d_{sd} from relay to destination as :

$$V_D = \frac{d_R}{d_{sd}}. \tag{3.15}$$

Also, we assume the relay is moving on the line parallel to the source-destination link with a destination d_R. The V_D is set from 0 to 1, which means the largest V_D is same as the distance from the source to the destination.

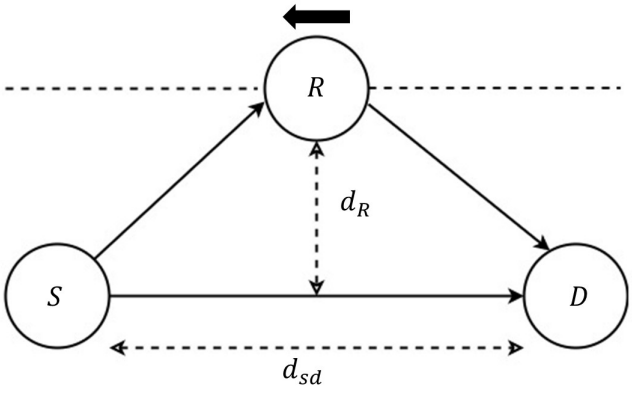

Figure 3.5: The system model of the different relay location

3.5 Exact Outage Probability Calculation for PLF system

Since all the three links are under independent block Rayleigh fading, the probability density function of $S-R$ link, $R-D$ link and $S-D$ link are independent, which means the joint *pdf* of the three links $p(\gamma_0, \gamma_1, \gamma_2)$ can be expressed as :

$$p(\gamma_0, \gamma_1, \gamma_2) = p(\gamma_0) \cdot p(\gamma_1) \cdot p(\gamma_2). \tag{3.16}$$

Then according to (3.4) and (3.10), the outage probability $P_{out}^{C_2}$ can be expressed as the addition of $P_{1,a}, P_{2,a}, P_{2,a}, P_{2,b}$.($P_{out}^{C_1} = P_{1,a}+P_{2,a}+P_{2,a}+P_{2,b}$)

And the $P_{1,a}, P_{2,a}, P_{2,b}, P_{2,b}$ are

$$\begin{aligned}
P_{1,a} &= Pr\left\{p=0, R_2 \geq 1, 0 \leq R_1 \leq H_b(p)\right\} \\
&= Pr\left\{\gamma_0 \geq \Phi_1^{-1}(1), \gamma_2 \geq \Phi_2^{-1}(1), \Phi_1^{-1}(0) \leq \gamma_1 \leq \Phi_1^{-1}(0)\right\} \\
&= \int_{\Phi_1^{-1}(0)}^{\Phi_1^{-1}(1)} d\gamma_0 \int_{\Phi_2^{-1}(0)}^{\Phi_2^{-1}(1)} d\gamma_2 \int_{\Phi_1^{-1}(0)}^{\Phi_1^{-1}(1)} p(\gamma_0)\cdot p(\gamma_1)\cdot p(\gamma_2) d\gamma_1 \\
&= 0
\end{aligned} \tag{3.17}$$

$$\begin{aligned}
P_{1,b} &= Pr\left\{p=0, 0 \leq R_2 \leq 1, 0 \leq R_1 \leq H_b(\alpha * p)\right\} \\
&= Pr\left\{\gamma_0 \geq \Phi_1^{-1}(1), \Phi_2^{-1}(0) \leq \gamma_2 \leq \Phi_2^{-1}(1), \Phi_1^{-1}(0) \leq \gamma_1 \leq [1-\Phi_2(\gamma_2)]\right\} \\
&= \int_{\Phi_1^{-1}(0)}^{\Phi_1^{-1}(\infty)} d\gamma_0 \int_{\Phi_2^{-1}(0)}^{\Phi_2^{-1}(1)} d\gamma_2 \int_{\Phi_1^{-1}(0)}^{\Phi_1^{-1}[1-\Phi_2(\gamma_2)]} p(\gamma_0)\cdot p(\gamma_1)\cdot p(\gamma_2) d\gamma_1 \\
&= \frac{1}{\Gamma_2}\exp\left[-\frac{\Phi_1^{-1}(1)}{\Gamma_0}\right] \int_{\Phi_2^{-1}(0)}^{\Phi_2^{-1}(1)} \exp(-\frac{\gamma_2}{\Gamma_2}) \cdot \left[1-\exp(-\frac{\Phi_1^{-1}\left[1-\Phi_2(\gamma_2)\right]}{\Gamma_1})\right] d\gamma_2
\end{aligned} \tag{3.18}$$

$$\begin{aligned}
P_{2,a} &= Pr\left\{0 < p \leq p_{th}, 0 \leq R_2 \leq 1, 0 \leq R_1 \leq H_b(p)\right\} \\
&= Pr\left\{\gamma_{th} \leq \gamma_0 \leq \Phi_1^{-1}(1), \gamma_2 \geq \Phi_2^{-1}(1), \Phi_1^{-1}(0) \leq \gamma_1 \leq [1-\Phi_1(\gamma_0)]\right\} \\
&= \int_{\gamma_{th}}^{\Phi_1^{-1}(1)} d\gamma_0 \int_{\Phi_2^{-1}(0)}^{\Phi_2^{-1}(\infty)} d\gamma_2 \int_{\Phi_1^{-1}(0)}^{\Phi_1^{-1}[1-\Phi_1(\gamma_0)]} p(\gamma_0)\cdot p(\gamma_1)\cdot p(\gamma_2) d\gamma_1 \\
&= \frac{1}{\Gamma_0}\exp\left[-\frac{\Phi_2^{-1}(1)}{\Gamma_2}\right] \int_{\gamma_{th}}^{\Phi_1^{-1}(1)} \exp(-\frac{\gamma_0}{\Gamma_0}) \cdot \left[1-\exp(-\frac{\Phi_1^{-1}\left[1-\Phi_1(\gamma_0)\right]}{\Gamma_1})\right] d\gamma_0
\end{aligned} \tag{3.19}$$

$$\begin{aligned}
P_{2,b} &= Pr\left\{0 < p \leq p_{th}, 0 \leq R_2 \leq 1, 0 \leq R_1 \leq H_b(\alpha * p)\right\} \\
&= Pr\left\{\gamma_{th} \leq \gamma_0 \leq \Phi_1^{-1}(1), \gamma_2 \geq \Phi_2^{-1}(1), \Phi_1^{-1}(0) \leq \gamma_1 \leq \Phi_1^{-1}\left[\Psi(\gamma_0,\gamma_2)\right]\right\} \\
&= \int_{\gamma_{th}}^{\Phi_1^{-1}(1)} d\gamma_0 \int_{\Phi_2^{-1}(0)}^{\Phi_2^{-1}(\infty)} d\gamma_2 \int_{\Phi_1^{-1}(0)}^{\Phi_1^{-1}[\Psi(\gamma_0,\gamma_2)]} p(\gamma_0)\cdot p(\gamma_1)\cdot p(\gamma_2) d\gamma_1 \\
&= \frac{1}{\Gamma_0\Gamma_2} \int_{\gamma_{th}}^{\Phi_1^{-1}(1)} \int_{\Phi_2^{-1}(0)}^{\Phi_2^{-1}(1)} \exp(-\frac{\gamma_0}{\Gamma_0} - \frac{\gamma_2}{\Gamma_2}) \cdot \left[1-\exp(-\frac{\Phi_1^{-1}\left[\Psi(\gamma_0,\gamma_2)\right]}{\Gamma_1})\right] d\gamma_0 d\gamma_2,
\end{aligned} \tag{3.20}$$

with

$$\Psi(\gamma_0,\gamma_2) = H_b\left\{H_b^{-1}\left[1-\Phi_1(\gamma_0)\right] * H_b^{-1}\left[1-\Phi_2(\gamma_2)\right]\right\}, \tag{3.21}$$

$$\Phi(\gamma) = \frac{\log_2(1+\gamma)}{R_s}. \tag{3.22}$$

Also, the $P_{out}^{C_1}$ can be expressed as:

$$\begin{aligned} P_{th} &= Pr\left\{p_{th} < p \leq 0.5, 0 \leq R_1 \leq H_b(p)\right\} \\ &= Pr\left\{\Phi_1^{-1}(0) \leq \gamma_0 \leq \gamma_{th}, \Phi_1^{-1}(0) \leq \gamma_1 \leq \Phi_1^{-1}(1)\right\} \\ &= \int_{\Phi_1^{-1}(0)}^{\gamma_{th}} d\gamma_0 \int_{\Phi_2^{-1}(0)}^{\Phi_2^{-1}(1)} p(\gamma_0) \cdot p(\gamma_1) \cdot p(\gamma_2) d\gamma_1 \\ &= \frac{1}{\Gamma_0 \Gamma_1} \int_{\Phi_1^{-1}(0)}^{\gamma_{th}} \int_{\Phi_2^{-1}(0)}^{\Phi_2^{-1}(1)} \exp(-\frac{\gamma_0}{\Gamma_0} - \frac{\gamma_1}{\Gamma_1}) d\gamma_0 d\gamma_1, \end{aligned} \tag{3.23}$$

The total P_{out}^{C} is :

$$P_{out}^{C} = P_{out}^{C_1} + P_{out}^{C_2}, \tag{3.24}$$

3.6 Numerical Results

3.6.1 Theoretical Results

In this section, theoretical outage probabilities of Lossy-Forwarding System(LF System) and PLF System are provided. Moreover, the outage probabilities comparison will include the different location of the relay and the vertical distance from the relay to the Source-Destination link. We use $dr = d_{sr}/d_{sd}$ to denote the distance ratio of the location of the relay, the way relay moves is introduced in section 2 Chapter 2. The geometric gains are calculated according to (2.1) and (2.2), with path-loss factor α.(α is setting as 3.52 in [11]) In Fig.3.6, by fixing $dr = 0.5$, we can see that the outage probability will increase when the instantaneous of γ_{th} is increasing. That is because if γ_{th} is larger, more bits will be discarded by relay.

In Fig.3.7, under the premise that the S-D link conditions remain unchanged, when the relay is getting close to the source, the average SNR of S-R link Γ_0 is decreasing. On the contrary, the probabilities which the instantaneous SNR of S-R link γ_0 is over than the setting threshold γ_{th} is increasing. Therefore, more bits discarded by the relay, the more outage increasing will be obtained. On the other hand, when relay is moving to the destination, the the average SNR of S-R link Γ_0 is increasing. Most bits will pass the threshold and be forwarded by the relay. That is why the gap between setting threshold or not is narrowing while the relay is moving to the destination.

Also, if we set an accurate outage probability called 'reliable outage boundary', which means the outage is acceptable only when it is below the boundary. And the area when the outage is below the boundary is called

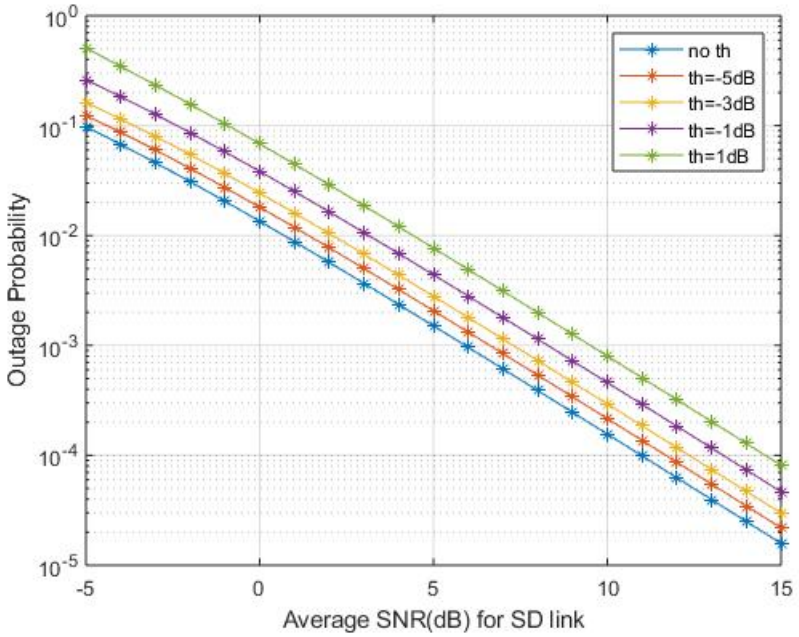

Figure 3.6: Comparisons of theoretical outage probabilities in different threshold

'Searching Area'(SA). In Fig.3.7 , the SA for Lossy-Forwarding System is $a-b$ and for PLF system is $c-d$. Obviously, the Searching Area is shrinking due to the setting of the threshold. Although the outage performance is relatively worse when setting threshold, it also benefits on energy efficiency. As (3.14) define, the energy efficiency η_{th} will be saved in PLF system.
As shown in Fig. 3.8. and Fig. 3.9. The energy efficiency is increasing when γ_{th} is decreasing, or the relay is close to the relay, which means more bits are discarded by the relay. From $\gamma_{th} = -5$dB to $\gamma_{th} = -1$dB, up to 17% 40% energy is saved.
Also, as shown in Fig.3.10 , the average SNR for $S-D$ link Γ_1 is set to 1dB. Obviously, when the relay is at the same position, the lower average SNR_{SD} can save more energy. On the other hand, the threshold setting will work well will in the low SNR area.
Fig. 3.11, Fig. 3.12 and Fig. 3.13 shows the result if we consider the vertical distance from Relay to distance V_D as a parameter. The definition of V_D is in section 3.4. As shown in Fig. 3.10, with same threshold, the outage probability will increase when the V_D is increasing, which means relay is moving away from the source and destination vertically. In Fig. 3.11, the Searching Area is shrinking from $a-d$ to $c-b$ when setting threshold, and

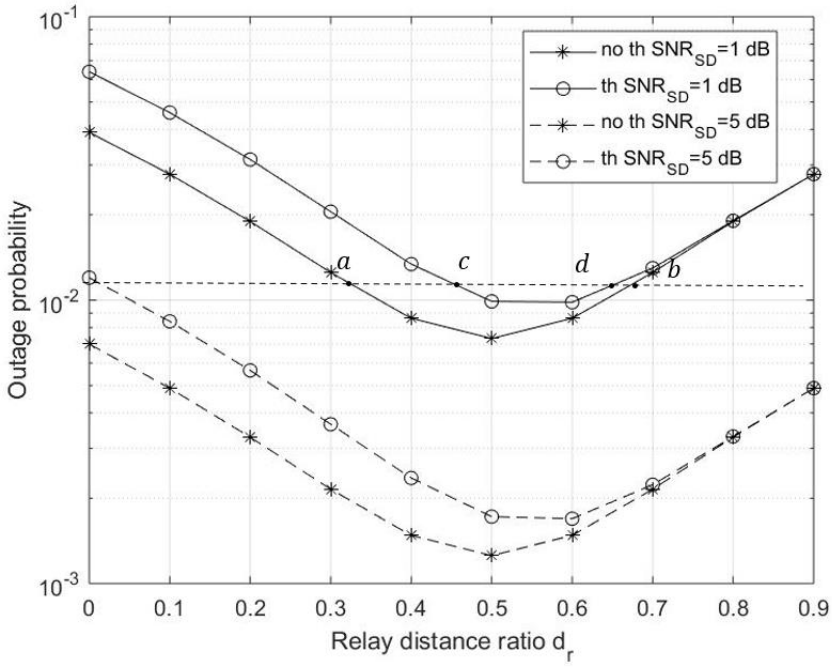

Figure 3.7: Comparisons of communication coverage with $\gamma_{th} = 0dB$

the area will be shrunk again from $c-b$ to $e-f$ when setting threshold and considering V_D. It is because the $S-R$ link is weaker when considering V_D and then more bits will be discarded by the relay. On the contrary, more energy will be saved as shown in Fig. 3.12.

3.6.2 Simulation Results

The chain simulation is under the condition that all three links are suffering from block-fading. The setting of chain simulation parameters is shown in Table. 3.1. Also, rather than using bit-flipping model in $S-R$ link, we assume this link also suffer fading to make the research more practical.
In Fig. 3.14, we can find out that FER will increase with the increment of the threshold γ_{th}.
In Fig. 3.15, we can clearly see the gap between the theoretical outage and practical outage. The optimal position to yield lowest outage is 0.4 rather than 0.5. That is because we assume $S-R$ link use the code which can achieve the channel capacity, but in practical, it can not achieve channel capacity, which makes the outage performance is worse than theoretical. To fix up this problem, the relay need to move closer to the relay to obtain more geometric gain from $S-R$ link.

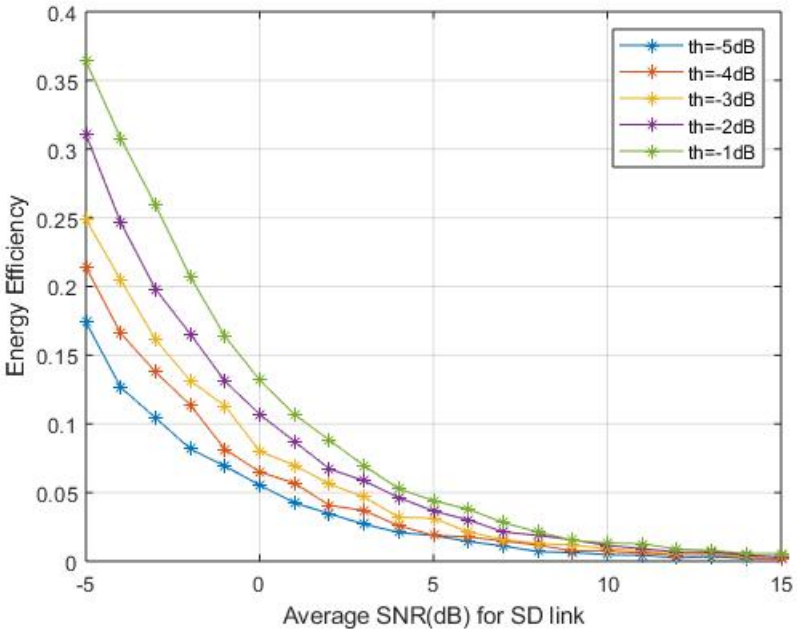

Figure 3.8: Comparisons of energy efficiency in different threshold

3.7 Summary of this Chapter

In this Chapter, we introduce the PLF system model firstly. Then according to Shannon's lossy source-channel separation theorem, we build the connection between intra-link error p and the instantaneous SNR for $S-R$ link γ_0. Then, according to the theorem for source coding with side information, we find the region where outage probability happens. To calculate the region by numerical integration, we find the theoretical outage probability will increase within threshold. Also, the communication coverage will be decreased. Then, after chain-simulation, we verify the conclusion above and calculate the energy efficiency saving from PLF technique. To compaste the geometric loss, then we introduce the vertical distance H. By considering H, we find that the energy efficiency will increase more although communication coverage will also decrease more.

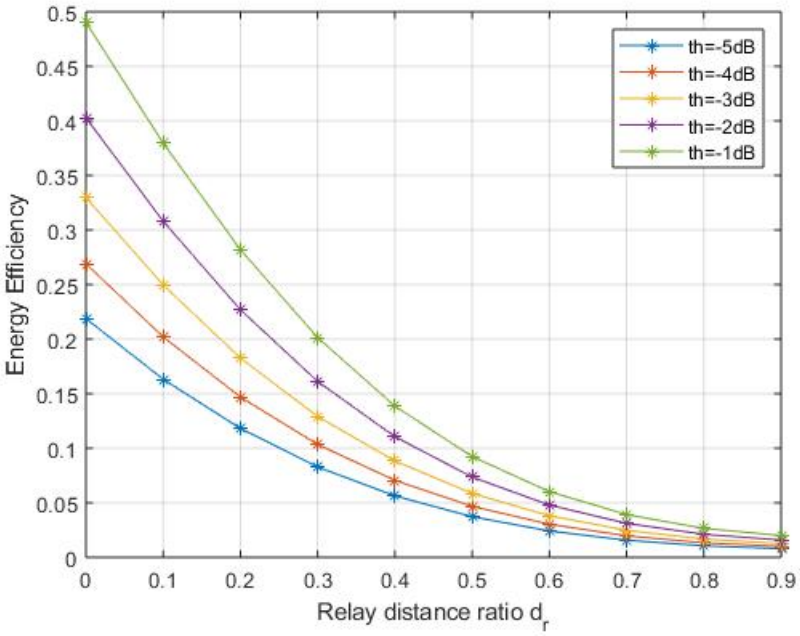

Figure 3.9: Comparisons of different threshold in theoretical outage probabilities with average SNR for S-D link is 1dB

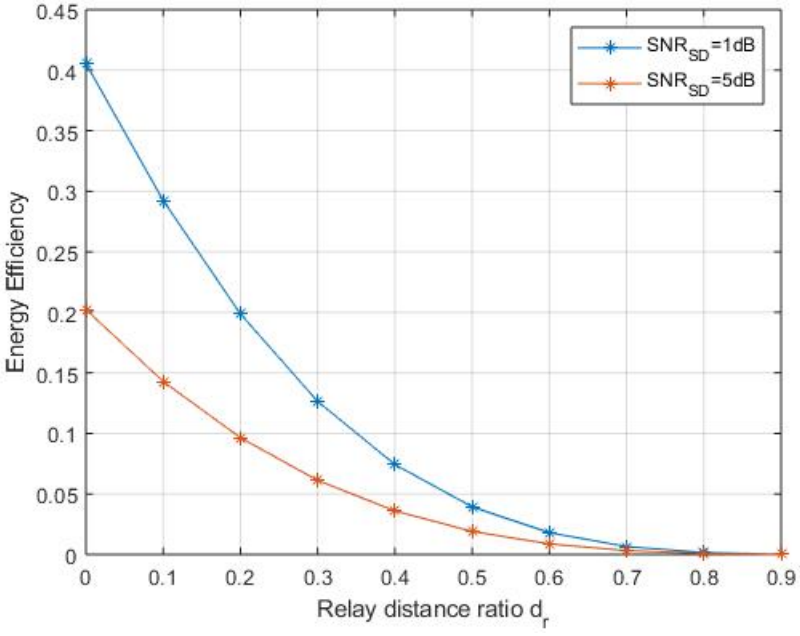

Figure 3.10: Comparisons of different average SNR for S-D link with γ_{th}=0dB

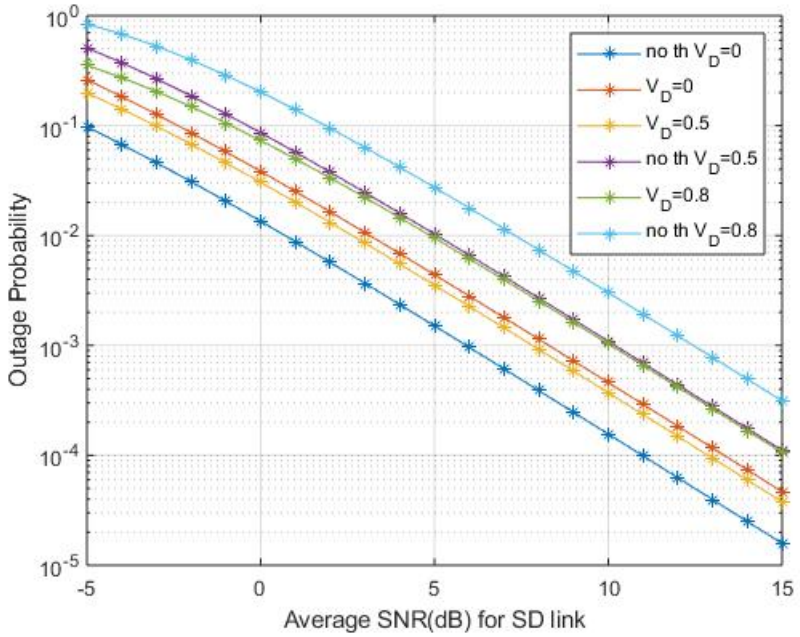

Figure 3.11: Comparisons of theoretical outage probabilities in different Vertical Distance with γ_{th}=0dB

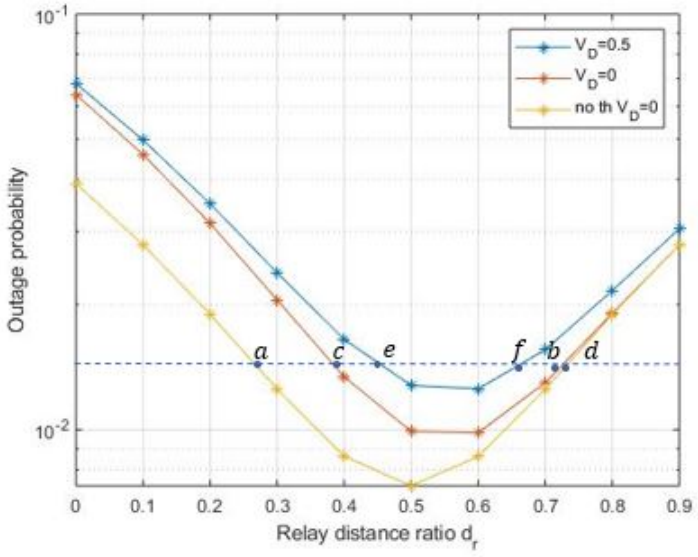

Figure 3.12: Comparisons of communication coverage in different Vertical Distance with average SNR for S-D link is 1dB and γ_{th} =0dB

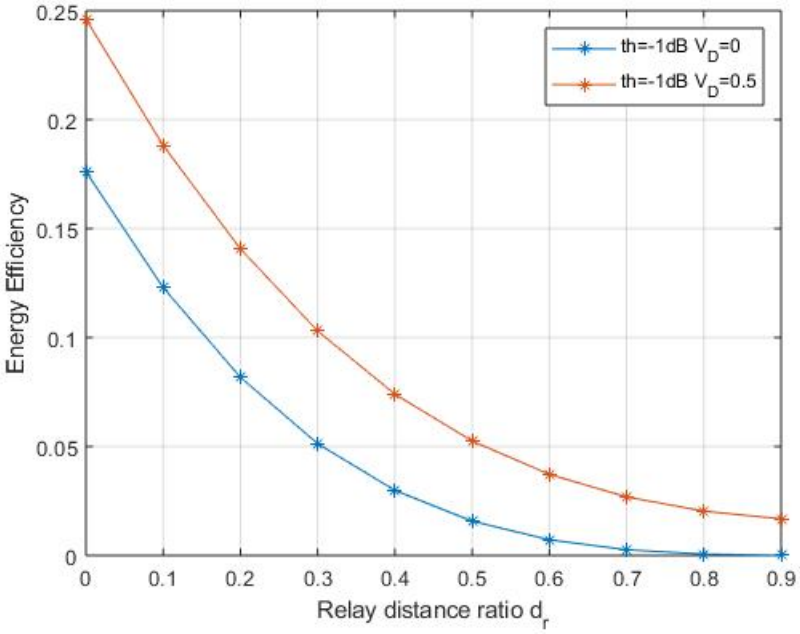

Figure 3.13: Comparisons of theoretical energy efficiency in different Vertical Distance with average SNR for S-D link is 1dB and γ_{th} =0dB

Item	Setting
u	$\Pr(u=0)=\Pr(u=1)=0.5$
Information sequence length N	10^4 bits
Decoding algorithm	BCJR
Encoder C_1	Rate $1/2$ $memory-1$ systematic non-recursive convolutional code
Encoder C_2	Rate $1/2$ $memory-1$ systematic recursive convolutional code
Modulation	QPSK
Channel Model	Block-rayleigh fading Channel
Iteration times	20

Table 3.1: The settings of chain simulation parameters

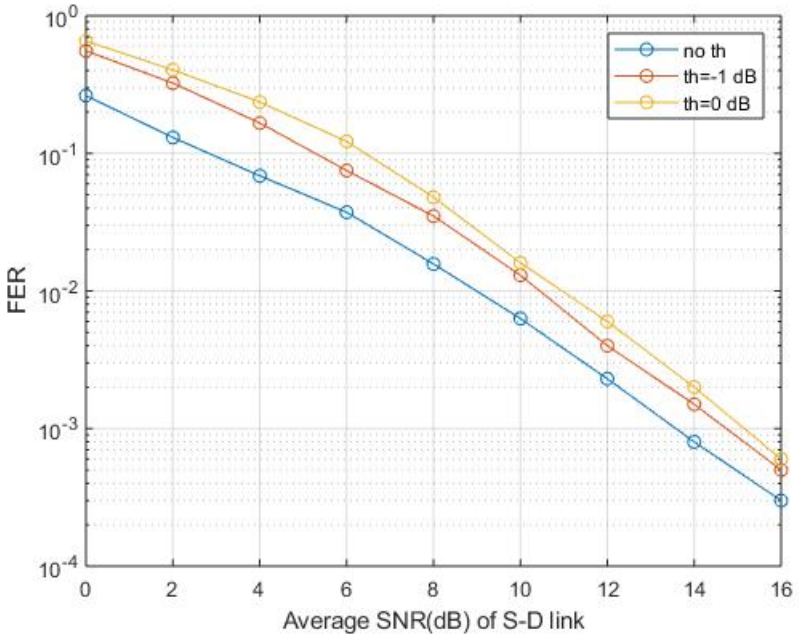

Figure 3.14: Comparisons of FER in LF and PLF System

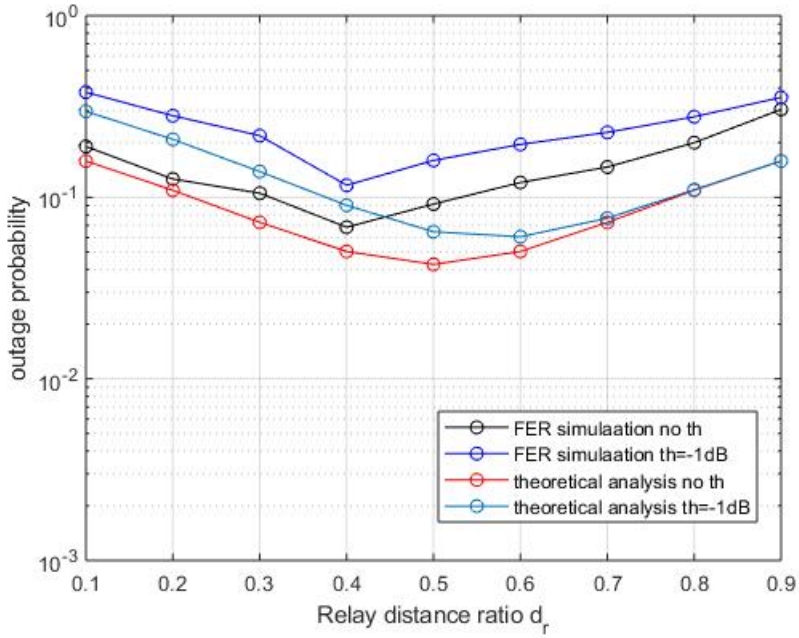

Figure 3.15: Comparisons of theoretical outage probabilities and practical FER with average SNR for S-D link is 0dB

Chapter 4

Exit-based Link Adaptation

In this chapter, we apply EXIT-based Link Algorithm to the single-relay system. We will introduce the basic knowledge for EXIT analysis and constellation constrained capacity firstly, then the principle of EXIT-based Link Algorithm will be introduced. Finally, based on that algorithm, the theoretical and practical outage probability will be shown.

4.1 Basics for EXIT analysis

In 2001, Stephan ten Brink introduced the EXIT chart [20], which describes the flow of extrinsic information between the decoders and visualize how the information about the transmitted coded bits gained by exchanging the likelihood ratio. By using EXIT charts, only the mutual information exchanged between demapper(or decoder, equalizer, etc) and decoder needs to be tracked rather than various variables. In this chapter, we use EXIT-chart to design the EXIT-based Link Adaptation Algorithm to select code rate and modulation method for $R - D$ link.

For example, we consider a receiver with demapper and decoder in the BICM-ID system as Fig 4.1. shows. In this system, the input of the demapper is the received signal from the channel L_y(in likelihood ratio, same below) and extrinsic information of the channel decoder L_A^2. And the out put of the demapper L_E^1 is a function of the received signal and the priori information provided by the channel decoder which is in the demapper.

$$L_E^1 = f(L_A^1, L_y). \tag{4.1}$$

Also the output of the decoder is a function of the demapper's output.

$$L_E^2 = f(L_A^1). \tag{4.2}$$

In [20], two observations have been found by the iterative decoding simulation as:

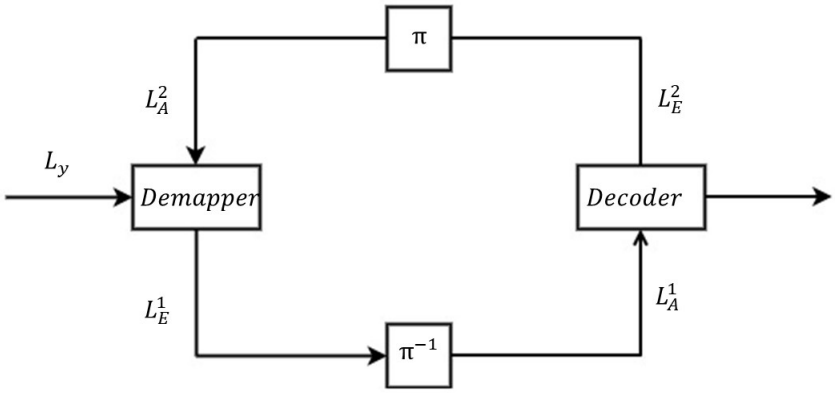

Figure 4.1: The system model of the BICM-ID System

- For larger interleavers, the priori values L_A remain fairly uncorrelated from the respective channel observations over many iterations.
- The *pdf* of extrinsic output values L_E, which is also equal to the priori values L_A approach the Gaussian distributions when the iterations times is increasing.

Then, we assume the L_A is modeled by introducing equivalent Gaussian channel, x is the transmitted information bit, suffering from independent Gaussian random noise n with the variance σ_A^2. Then L_A can be expressed as:

$$L_A = \mu_A \cdot X + n, \tag{4.3}$$

where n denotes the independent Gaussian random noise. Since L_A is assumed to be an L-value of a Gaussian channel output, the mean value μ_A must satisfies :

$$\mu_A = \frac{\sigma_A^2}{2}. \tag{4.4}$$

Then, for each bit x in sequence X the mutual information $I(X;A)$ between the demapper and the decoder is:

$$
\begin{aligned}
I(X;A) &= H(X) - H(X \mid A) \\
&= \sum_{x \in X} \int_{\lambda \in A} p(X,A) \log \frac{p(X,A)}{p(X)p(A)} d\lambda \\
&= \sum_{x \in X} \int_{\lambda \in A} p(X,A) \log \frac{p(A \mid X)p(X)}{p(X)p(A)} d\lambda \\
&= \sum_{x \in X} \int_{\lambda \in A} p(A \mid X)p(X) \log \frac{p(A \mid X)}{p(A)} d\lambda \\
&= \sum_{x=1} \int_{-\infty}^{\infty} p_A(\lambda \mid X = x) \frac{1}{2} \log \frac{p_A(\lambda \mid X = x)}{p_A(\lambda)} d\lambda. \qquad (4.5)
\end{aligned}
$$

Here, $p_A(\lambda|X = x)$ is the probability of the LLR being λ conditioned of the sequence X. The conditional probability density function is:

$$
p_i(\lambda \mid X = x) = \frac{1}{\sqrt{2\pi}\sigma_A} \exp\left(- \frac{\left(\lambda - \frac{\sigma_A^2}{2} x\right)^2}{2\sigma_A^2} \right). \qquad (4.6)
$$

Then, the mutual information $I(X;A)$, which can be written as $I_A(\sigma_A)$ when the σ_A is given, can be expressed by:

$$
\begin{aligned}
I_A(\sigma_A) &= \frac{1}{2} \sum_{x=+1,-1} \int_{-\infty}^{\infty} p_i(\lambda \mid X = x) \log_2 \left[\frac{2p_i(\lambda \mid X = x)}{p_i(\lambda \mid X = -1) + p_i(\lambda \mid X = +1)} \right] d\lambda \\
&= 1 - \int_{-\infty}^{\infty} \frac{1}{\sqrt{2\pi}\sigma_i} \exp\left[- \frac{\left(\lambda - \frac{\sigma_i^2}{2} x\right)^2}{2\sigma_i^2} \right] \log_2[1 - \exp(-\lambda)] d\lambda. \qquad (4.7)
\end{aligned}
$$

To simplify the process, we use the approximated J-Function to express I_A :

$$
\begin{aligned}
I_A &= J(\sigma_A) \\
&\approx (1 - 2^{-H_1 \sigma^{2H_2}})^{H_3}, \qquad (4.8)
\end{aligned}
$$

where $H_1 = 0.3073$,$H_2 = 0.8935$,$H_3 = 1.1064$. [21] Those parameters are calculated by curve fitting based on lease-squared. Also, we can obtain the variable I_A according to mutual information as shown in:

$$
\begin{aligned}
\sigma_A &= J^{-1}(I_A) \\
&\approx \left(- \frac{1}{H_1} \log_2 \left(1 - I^{\frac{1}{H_3}} \right) \right)^{\frac{1}{2H_2}}. \qquad (4.9)
\end{aligned}
$$

However, if the variance σ_A can not be obtained, we can also calculate the mutual information of the soft input soft out put demapper I_E by calculating the histogram of the LLR.

$$\begin{aligned} I_E &= I(L_E; X) \\ &= \frac{1}{2} \sum_{x=+1,-1} \int_{-\infty}^{\infty} p_i(\lambda \mid X = x) \\ &\quad \log_2 \left[\frac{2p_i(\lambda \mid X = x)}{p_i(\lambda \mid X = -1) + p_i(\lambda \mid X = +1)} \right] d\lambda. \end{aligned} \tag{4.10}$$

4.2 EXIT charts for Outer Codes

To visualize how the mutual information exchanged from the demapper and the decoder in the EXIT-chart, the x and y axis for the outer code are flipped since the output of the channel decoder is the input of the demapper, vice versa. To calculate the outer code only, we divided the BICM-ID system into two parts and input the I_A manually from 0 to 1. The outer code EXIT-chart, which use [15 17](generators in octal) in half rate code, is shown in Fig.4.2.

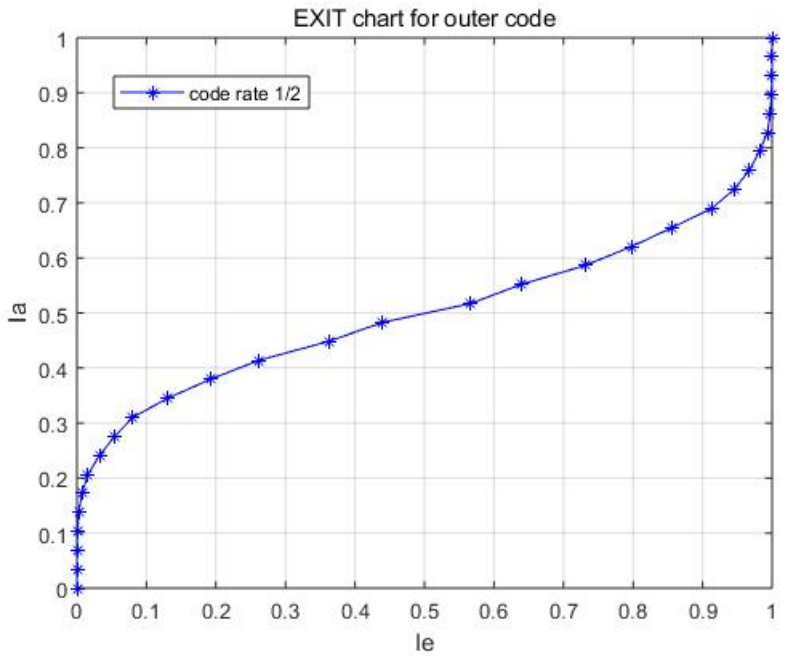

Figure 4.2: Convolutional Codes with 1/2 code rate

4.3 EXIT Charts for Inner Codes

4.3.1 Area Property

In [22], we can obtain that the area E under the demapper EXIT curve is corresponding to the constellation constrained capacity. And if the EXIT function of the posteriori information of the outer decoder output does not intersect with the inner code curve, the area under the decoder EXIT curve(lower curve) is equal to the rate r_c of the code. Generally, if the demapper curve and the decoder curve does not intersect with each other, the area E is the same as the channel capacity. Under this condition, if the rate of the outer code is smaller than the constellation constrained capacity and the received sequence can be iteratively decoded without any error.

4.3.2 EXIT charts in different Mapping rules

The shape of the EXIT curve strongly depends on the constellation diagram. It is found that all the standard mapping schemes with different arrangement of the labels have the same area under the EXIT curve, since the constellation constrained capacity is not dependent on the labeling rule which is used.
As an example, we introduce three different constellation mapping rules, which is $Gray$ Mapping, $M16^a$ Mapping, and Modified Set Partitioning(MSP) Maping. Then, the EXIT-curve of the three different Mapping rules will be obtained to explain the difference in Inner Code curve between different mapping rules.
For all the three Mapping each label has a length $l_{map} = log_2(M)$, where M is the signal points per symbol in the constellation diagram, in 16 Quadrature Amplitude Modulation (QAM), M=4.
In [23], the distance spectrum is mentioned as a method to evaluate the performance for different mapping rules. It is defined as the number $N(d_E)$ of symbols in the constellation diagram(X) $s_i \epsilon x_b^p$, with the Euclidean distance d_E from the symbol $s_i \epsilon x_b^p$, where the x_b^p is the subset of symbols whose bit label have the value b at the p^{th} position. The distance spectrum $N(d_E)$ is expressed as:

$$N(d_E) = \frac{\sum_{p=1}^{l_{map}} \sum_{b_p=0}^{l} \sum_{s_i \epsilon x_b^p} N_N(d_E, s_i)}{l_{map} \cdot 2^M}. \tag{4.11}$$

The result of distance spectrum distance is given in [24]. From the result, we can obtain that:

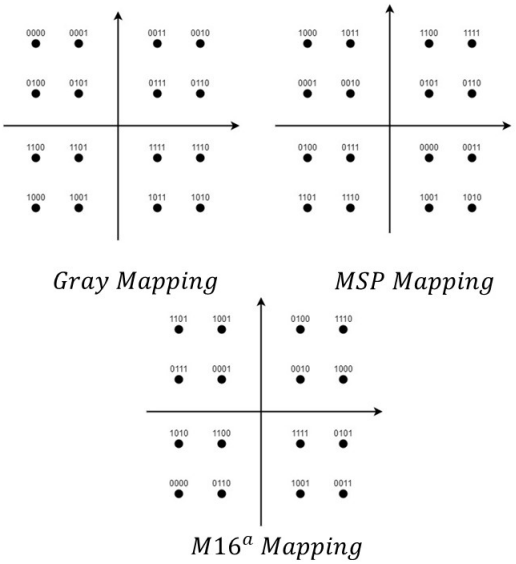

Figure 4.3: The Mapping rules for different 16QAM Mapping

- If the priori information is unavailable, which means demapper knows nothing about the information sequence, the *Gray* Mapping outperforms any other mapping schemes.
- On the contrary, if the priori information sequence approach the maximum value, which means demapper can obtain the full information from the information sequence, the *Gray* mapping performance is worst and the $M16^a$ Mapping is the best mapping scheme.
- The performance of MSP Mapping scheme is always between the *Gray* Mapping and $M16^a$ Mapping. Therefore, the MSP Mapping is a good choice between full and zero priori information

Then, as shown in Fig 4.4., with doping accumulator technique which is introduced in Chapter 2, all three EXIT-curve can reach (1,1) point in EXIT-chart.(To simplify calculation, the doping ratio is set as 2). For Gray mapping, beginning point is the highest. For $M16^a$ Mapping and the MSP Mapping, although the starting point is lower than Gray Mapping, they can also achieve (1,1) point finally under many iterations.(The trajectory is shown as green dotted lines in Fig 4.4.), which means the non-gray mapping can achieve better performance under massive iteration in even bad channel condition. Moreover, the MSP mapping have a better performance than $M16^a$ Mapping and the *Gray* Mapping.
Generally, for BICM-ID systems, although the Gray mapping have a higher staring point we will choose non-Gray mapping rules in Quadrature Phase

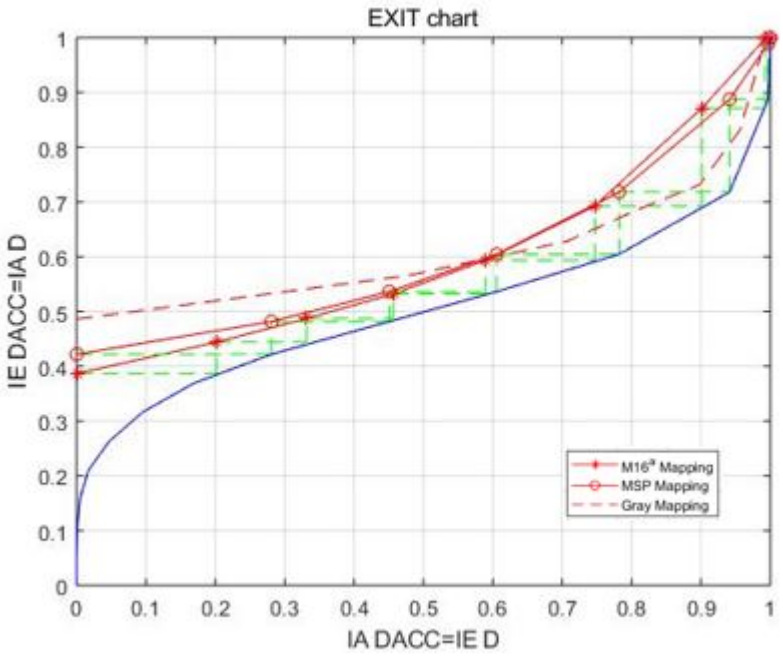

Figure 4.4: 16QAM with $\frac{E_S}{N_0}$ 8dB and code rate $\frac{1}{2}$ in different mapping rules

Shift Keying (QPSK) and 16-QAM in Link-Adaptation algorithm.

4.4 Constellation Constrained Capacity

Constellation Constrained Capacity of Simple-input-simple-output(SISO) has been fully studied in many literature. In [25], one-dimensional and two-dimensional modulation is considered in AWGN channel.
We assume z as the received signal which suffer from independent normally distributed noise sample with variance σ_2 and zero-mean.$P(z)$ represents the independent continuous distribution probability of the signal. $P(k)$ represents the prior discrete probability by $k-th$ information sequence.$P(k,z)$ denoted the joint distribution probability. From [25], we can obtain that under one-dimensional case, $P(z)$,$P(k)$, and $P(z,k)$ can be expressed as:

$$p(z) = \sum_{k=1}^{N} p(z,k) = \sum_{k=1}^{N} \frac{1}{N} \cdot \frac{\exp\left(\frac{-\left|z-n^k\right|^2}{2\sigma^2}\right)}{\sqrt{2\pi\sigma^2}}, \tag{4.12}$$

where we assume n^k is the $k-th$ channel signal point in the modulation.

$$p(k) = \int_{-\infty}^{\infty} p(z,k)dz = \frac{1}{N} \tag{4.13}$$

$$p(z,k) = \frac{\exp\left(\frac{-\left|z-a^k\right|^2}{2\sigma^2}\right)}{\sqrt{2\pi\sigma^2}} \cdot \left(\frac{1}{N}\right), \tag{4.14}$$

where N is assumed as the length of the signal points in different modulation. Also we assume $p(k)$ is uniform distribution and therefore $p(k)$ and $p(z)$ are independent. In the two dimensional case,

$$p(z) = \sum_{i=1}^{\sqrt{N}} \sum_{r=1}^{\sqrt{N}} \frac{1}{N} \left(\frac{\exp\left(\frac{-\left|x-a_r^k\right|}{2\sigma^2}\right)^2}{\sqrt{2\pi\sigma^2}} \right) \cdot \left(\frac{\exp\left(\frac{-\left|y-a_i^k\right|^2}{2\sigma^2}\right)}{\sqrt{2\pi\sigma^2}} \right) \tag{4.15}$$

$$p(k) = \int_{-\infty}^{+\infty} \int_{-\infty}^{+\infty} p(z,k)dxdy = \frac{1}{N} \tag{4.16}$$

$$p(z,k) = \left(\frac{1}{N}\right) \cdot \left(\frac{\exp\left(\frac{-\left|x-a_r^k\right|^2}{2\sigma^2}\right)}{\sqrt{2\pi\sigma^2}} \right) \cdot \left(\frac{\exp\left(\frac{-\left|y-a_i^k\right|^2}{2\sigma^2}\right)}{\sqrt{2\pi\sigma^2}} \right), \tag{4.17}$$

where a_r^k and a_i^k denotes the real component and the imaginary component of the $k-th$ signal.
Also, the channel capacity can be expressed as:

$$\begin{aligned} C &= \max_{p(k)} \mathrm{I(K;Z)} \\ &= \max_{p(k)} \sum_{k \epsilon K} \int_{-\infty}^{+\infty} p(z,k) log \frac{p(k,z)}{p(k)p(z)} dz, \end{aligned} \tag{4.18}$$

where the maximum value of Constellation Constrained Capacity (CCC) is $log_2(N)$ bits [26]. To simplify the calculation, (4.18) can also be written in (4.19) [25].

$$C = log_2 N - \frac{1}{N} \cdot \sum_{k=0}^{N-1} E\left\{ \log_2 \sum_{i=0}^{N-1} \exp\left[-\frac{|a^k + w - a^i| - |w|^2}{2\sigma^2} \right] \right\}, \tag{4.19}$$

We can obtain the CCC curve from (4.19) by Monte Carlo simulation, however, in order to calculate the rate loss easily in the following section,

we need an equation to approximate the CCC curves. In [27], we found the approximate equation as:

$$C_{BPSK} \approx \frac{1}{2}\log(1+\gamma) - \frac{1}{4}\log\left[1+\frac{\gamma^2}{M^4}\right] \tag{4.20}$$

$$C_{QPSK} \approx \log(1+\gamma) - \frac{1}{2}\log\left[1+\frac{\gamma^2}{M^2}\right] \tag{4.21}$$

$$C_{16QAM} \approx \log(1+\gamma) - \frac{1}{1.1}\log\left[1+\frac{\gamma^2}{M^{1.1}}\right], \tag{4.22}$$

where γ denotes the instantaneous SNR of the link and M denotes the length of the symbol in different modulation schemes(for Binary Phase Shift Keying (BPSK), M=1,for QPSK, M=2, for 16QAM, M=4). However, the approximation use standard mapping rules but we use non-Gray mapping rules in QPSK and 16QAM, there exists shapping loss difference between two mapping schemes. However, as seen in Fig 4.5, the difference between different mapping rules is minor. Therefore, we use (4.20-4.22) to calculate CCC in the following sections, called C_M functions.($C = C_M(\gamma)$).

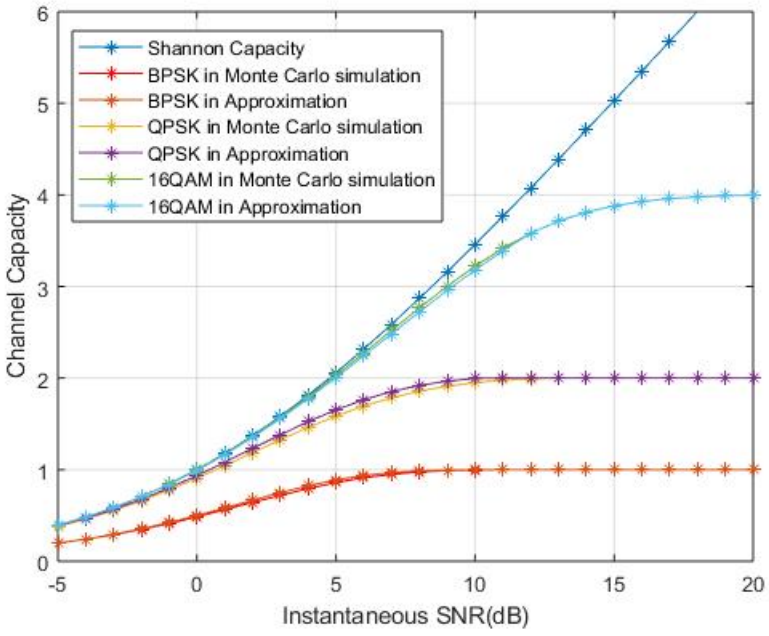

Figure 4.5: The Constellation Constrained Capacity for different Mapping rules

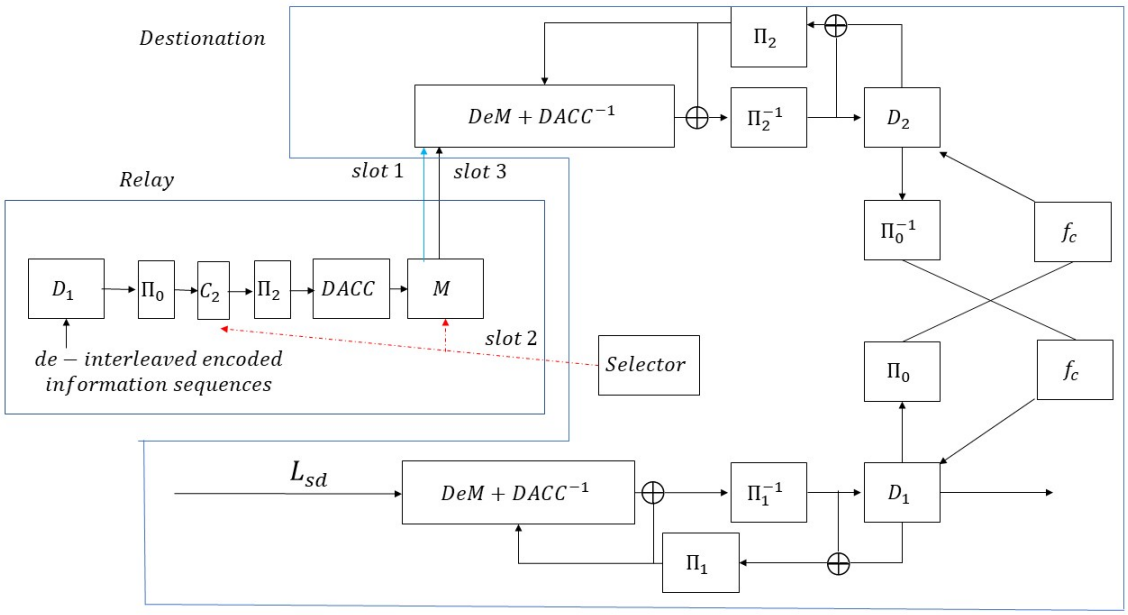

Figure 4.6: Link Adaptation for the LALFOR System where R-D link signaling parameters is specified by the protocol shown in Fig 4.7

4.5 EXIT-based Link Adaptation Algorithm

4.5.1 System Model

As shown in Fig 4.6. and Fig 4.7, we focused on the $Relay - Destination$ link($R - D$ link) in traditional three-relays Lossy Forwarding System. The BICM-ID technique, which is introduced in Section 2.3, is used to demodulate and decode the information sequences in the horizontal iterations. The joint-decoding is using in vertical iterations, which is introduced in Section 2.7. As mentioned in Chapter 2, the transmission process between relay and destination is divided into three slots in phase 2:

- phase 2 slot 1, relay use *precursor* technique to acquire the channel condition of $R - D$ link.
- phase 2 slot 2, according to the instantaneous SNR γ_2, the selector choose the modulation method and code rate as the feedback information to the relay.
- phase 2 slot 3, relay started sending information sequences to the destination.

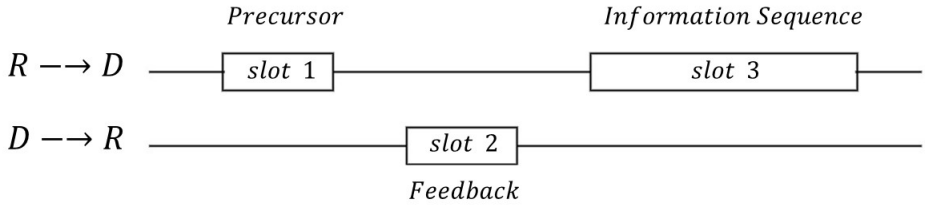

Figure 4.7: Transmission Protocol for R-D Link Adaptation of the LALFOR System

4.5.2 The principle of EXIT-based Link Adaptation Algorithm

As mentioned in the previous section, for the BICM-ID system, as shown in Fig 4.8., if the the two EXIT-curve intersect with each other due to the low average SNR, the mutual information between demapper and decoder can not get improved. On the contrary, if the demapper EXIT curve does not intersect with the decoder EXIT curve, the rate of the outer code which is smaller than the CCC and the received sequence can be decoded in error free iteratively. However, as shown in Fig 4.9., if the SNR is too large, the gap between demapper curve and decoder curve will become huge and the rate loss will also be huge.

Therefore, we should avoid those two situation in our EXIT-based Link Adaptation algorithm.For each Modulation Method M, we can draw different EXIT outer code rate curve from $\frac{1}{8}$ to $\frac{7}{8}$ and different EXIT inner code rate in each SNR. The generators of those codes are shown in Table 4.1: [28]
The set of the R-D link signaling parameters $L(i, j)$, which is specified by

Rate	Generators in octal	Puncturing Pattern
1/8	17 17 13 13 13 15 15 17	()
1/7	17 17 13 13 13 15 15	()
1/6	17 17 13 13 15 15	()
1/5	17 17 13 15 15	()
1/4	13 15 15 17	()
1/3	13 15 17	()
1/2	15 17	()
2/3	15 17	(11 10)
3/4	15 17	(11 10 01)
4/5	15 17	(11 01 10 10)
5/6	15 17	(11 01 10 01 01)
6/7	15 17	(11 01 01 01 10 10)
7/8	15 17	(11 01 01 01 01 10 01)

Table 4.1: The settings of generators and puncturing pattern

the destination via the feedback channel, is defined as:

$$L(i,j) = \Big(L(\frac{1}{8}, BPSK), L(\frac{2}{8}, BPSK), ..., L(\frac{7}{8}, BPSK), \\ L(\frac{1}{8}, QPSK), ..., L(R_c, \underline{M})\Big), \tag{4.23}$$

where R_c denotes the code rate and $\underline{M}$ denotes the modulation multiplicity . Then We find for each set $L(i,j)$ there exists instantaneous SNR $\gamma(R_c, \underline{M})$, which just let the convergence tunnel which is between two curves open, as shown in Fig 4.11. Then, we can obtain

$$\gamma(L_i) = \Big(\gamma(\frac{1}{8}, BPSK), \gamma(\frac{2}{8}, BPSK), ..., \gamma(\frac{7}{8}, BPSK), \\ \gamma(\frac{1}{8}, QPSK), ..., \gamma(R_c, \underline{M})\Big). \tag{4.24}$$

Then, to obtain real-code performance, we need to calculate the actual rate with the specified signaling parameters $L(R_c, \underline{M})$. It is defined as:

$$R(R_c, \underline{M}) = C_M(\gamma) - \Delta R, \tag{4.25}$$

where ΔR denotes the rate loss between the demapper and the decoder, which is shown as the gap between demapper curve and decoder curve in EXIT chart. It is equal to the size of the area between demapper and decoder.

We can calculate it by numerical integration (as an example, the gap area is the blue area in Fig 4.13.).Now, we can clearly identify the objective of the link adaptation, which is to determine the signaling parameters in (4.23) that minimize the rate loss ΔR using practical coding and modulation schemes.

4.5.3 The procedure of EXIT-based Link Adaptation Algorithm

Our proposed link adaptation algorithm is summarized as follows: for each frame, if the instantaneous SNR γ_2, which is obtained from the precursor technique, is smaller than $\gamma_{th}(\frac{2}{3}, BPSK)$, then the relay will choose $R_c = \frac{1}{2}$ and BPSK, if γ_2 is larger than $\gamma_{th}(\frac{2}{3}, BPSK)$ but smaller than $\gamma_{th}(\frac{3}{4}, BPSK)$, we will select $R_c = \frac{2}{3}$ and BPSK, ...,etc. The process of selecting code rate and modulation method with the proposed algorithm is shown in Algorithm 4.1. To simplify the calculation, the R_c is constrained from $\frac{1}{2}$ to $\frac{3}{4}$

Algorithm 4.1 EXIT-based Link Adaptation Algorithm

Input: $\gamma_{th}(R_c, \underline{M})$, γ_2
Output: $R_c^{'}$,$\underline{M}'$
set $R_c^{'} = 1/2$,$\underline{M}' = BPSK$;
if $\gamma_2 < \gamma_{th}(R_c = 2/3, \underline{M} = BPSK)$ **then**
  $R_c^{'} = 1/2$,$\underline{M}' = BPSK$;
else if $\gamma_{th}(R_c = 2/3, \underline{M} = BPSK) < \gamma_2 < \gamma_{th}(R_c = 3/4, \underline{M} = BPSK)$ **then**
  $R_c^{'} = 2/3$,$\underline{M}' = BPSK$;
else if $\gamma_{th}(R_c = 3/4, \underline{M} = BPSK) < \gamma_2 < \gamma_{th}(R_c = 1/2, \underline{M} = QPSK)$ **then**
  $R_c^{'} = 3/4$,$\underline{M}' = BPSK$;
else if $\gamma_{th}(R_c = 1/2, \underline{M} = QPSK) < \gamma_2 < \gamma_{th}(R_c = 2/3, \underline{M} = QPSK)$ **then**
  $R_c^{'} = 1/2$,$\underline{M}^{'} = QPSK$;
  ...
end if

where γ_2 denotes the instantaneous SNR of R-D link, $R_c^{'}$ and $\underline{M}^{'}$ denotes the selected code rate and modualtion method. Fig 4.12., shows the process of the algorithm on the CCC figure, where B denotes BPSK, Q denotes $QPSK$(non-Gray), and 16 denotes $16QAM(M16^a)$.

4.6 Numerical Results

Using equations from (3.24-3.26), we can calculate the theoretical outage probabilities for three-node Lossy Forwarding systems in different code rate and modulation schemes for $R-D$ link by selecting R_{c2} in $\Phi(\gamma)$ function in (3.22). As shown in Fig 4.14 and Fig 4.15, we can see that outage probabilities changes from the lowest set of the selected code rate and modulation method to the highest selected code rate and modulation method. It is mentioned that for $S-D$ link and $R-D$ link, the code rate is set as $1/2$ and modulation is set as QPSK.
Although the Link Adaptation technique make the performance worse, we can save throughput efficiency from this technique, which will be introduced in the next Chapter.

4.7 Summary of this Chapter

In this chapter, we introduce the principle of the EXIT chart and Constellation Constrained Capacity. After that, the principle and procedure of the EXIT-based adaptive transmission is provided. Finally, we obtained some numerical results to compare the FER between given parameters of code rate and modulation and adaptive transmission.

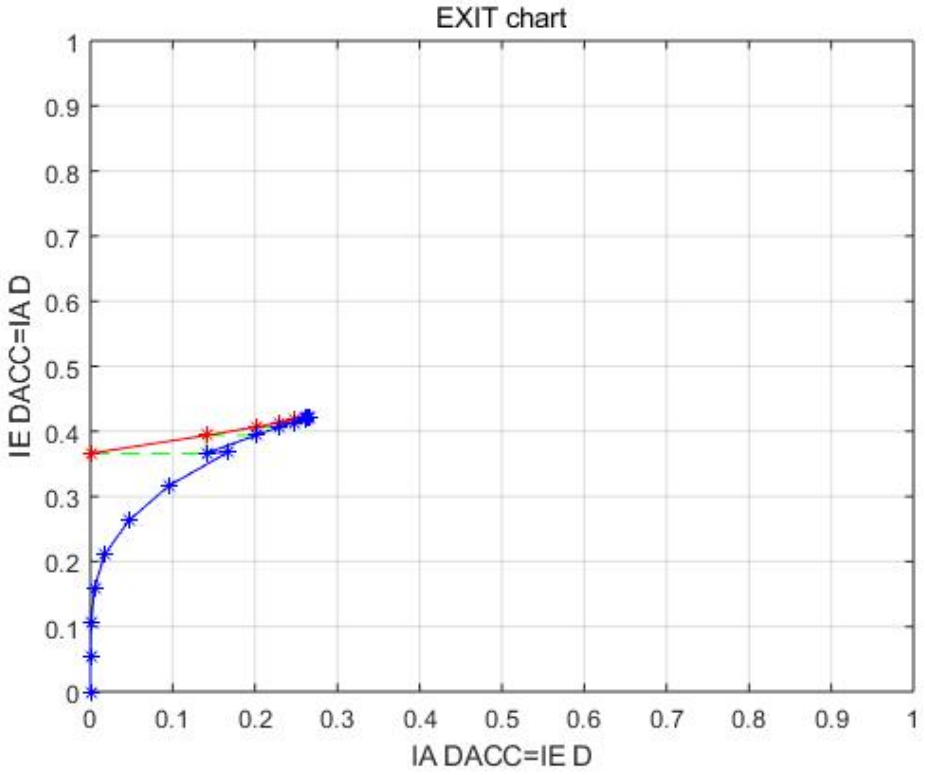

Figure 4.8: EXIT chart with code rate $R_c = 1/2$,BPSK,Eb/N0 1dB

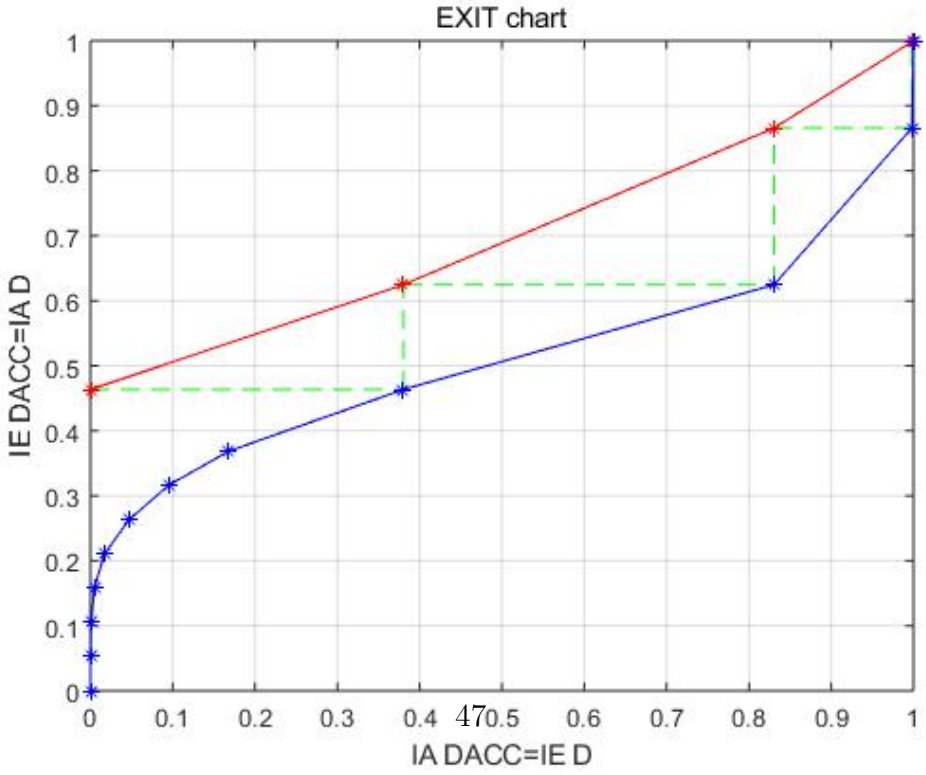

Figure 4.9: EXIT chart with code rate $R_c = 1/2$,BPSK,Eb/N0 6dB

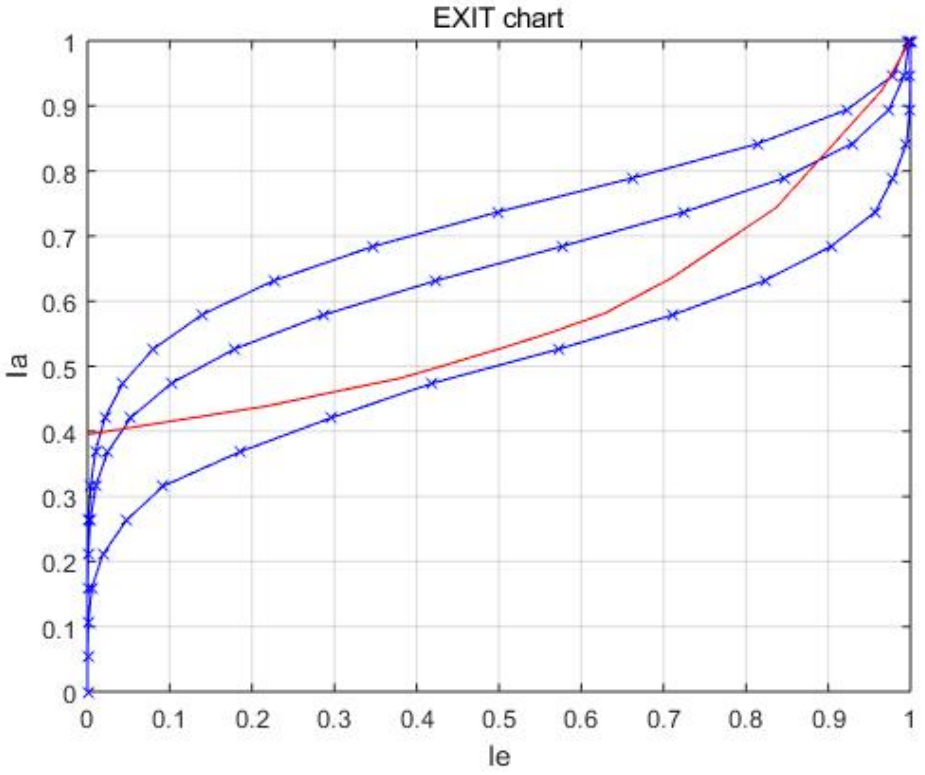

Figure 4.10: EXIT chart with code rate code rate from 1/2 to 3/4

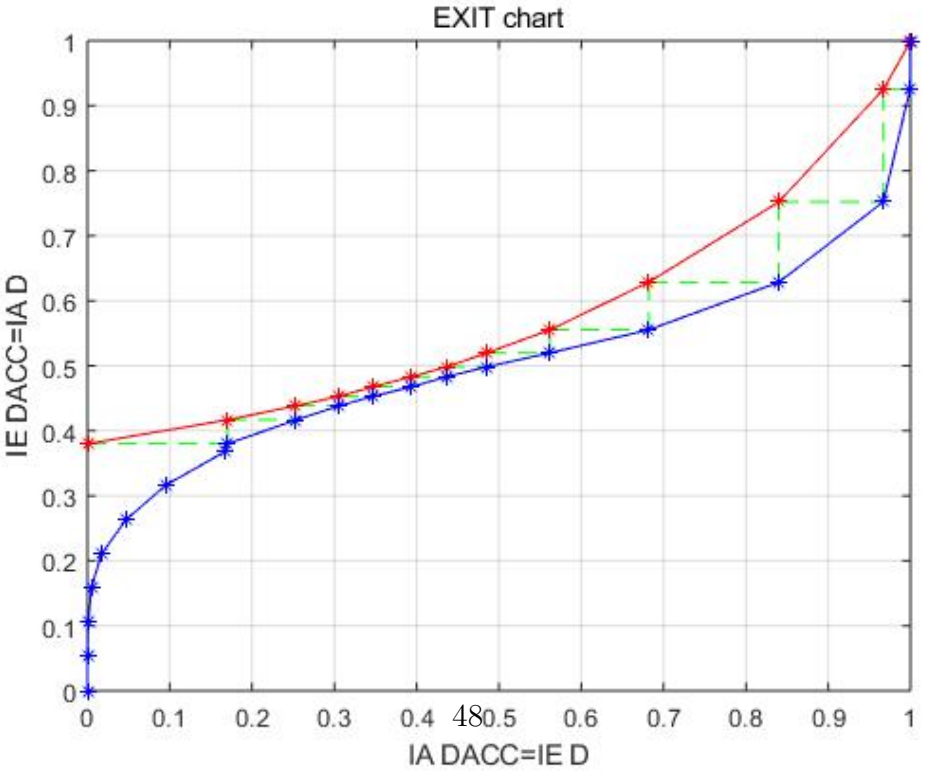

Figure 4.11: EXIT chart with code rate $R_c = 1/2$,BPSK,Eb/N0 3.25dB

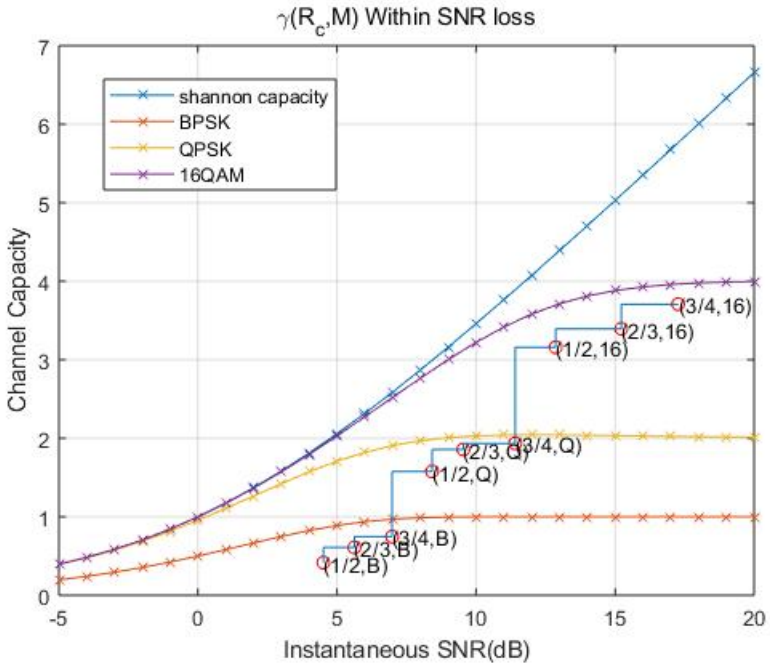

Figure 4.12: The trace for EXIT-based Link Adaptation Algorithm within SNR loss

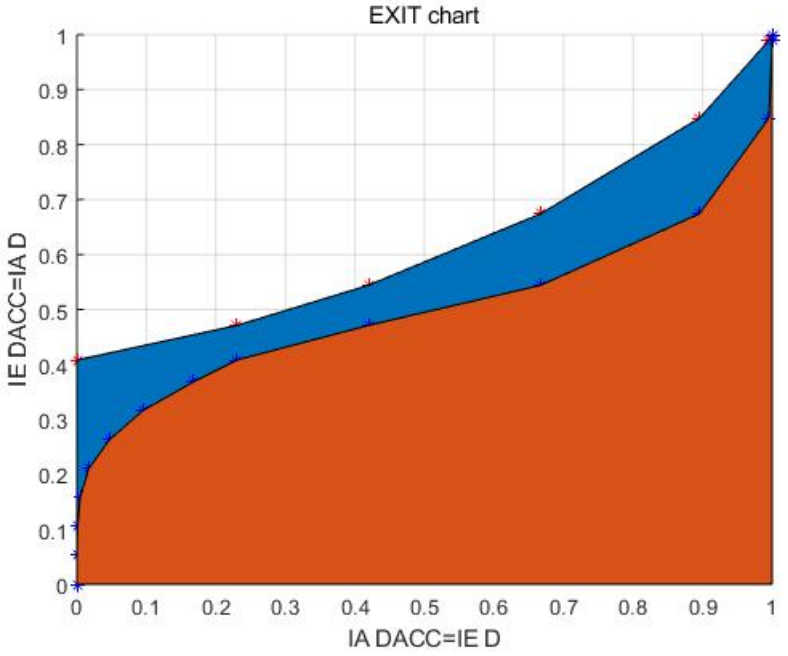

Figure 4.13: Rate-Capacity Relation of the EXIT chart

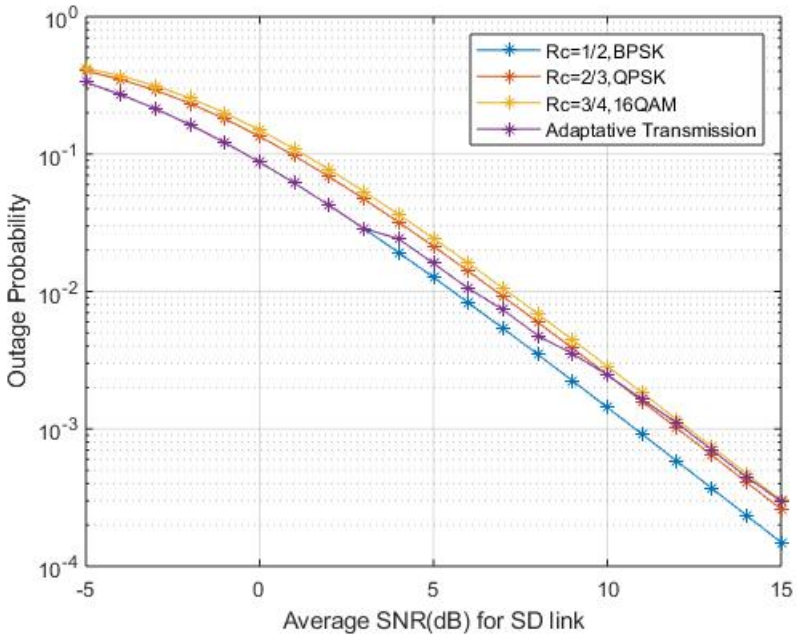

Figure 4.14: Outage Probabilities for different code rate and modulation

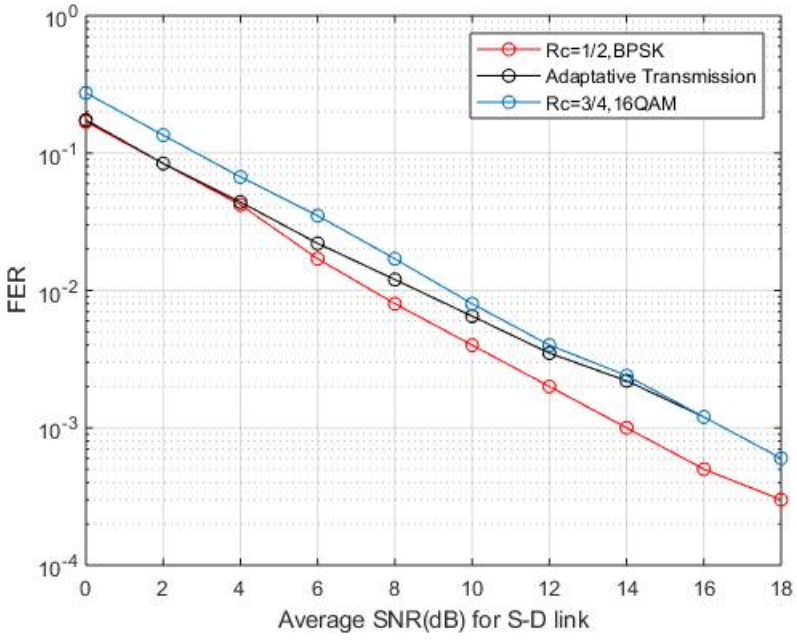

Figure 4.15: The comparison between Rc=1/2, BPSK and adaptive transmission over fading channel

Chapter 5

LALFOR System

In this chapter, we introduce the system model of LALFOR system, the definition of throughput efficiency time consuming firstly.Then we show the numerical results of throughput efficiency improvement and energy efficiency in different conditions.

5.1 System Model

As mentioned in Chapter 2, the principle of the LALFOR system is shown in Fig.5.1. In phase 1, the source broadcast the information sequences, to the relay and destination. After receiving information sequence from source, relay will make a destination to judge whether drop out or forward according to the channel condition of $S-R$ link. If the channel condition is bad, relay will discard the sequence. If the channel condition is good, relay will decoded the sequences and re-encoded it. In phase 2 slot 1, relay will acquire the channel capacity by precursor technique. In phase 2 slot 2, the selected code rate and modulation method, obtained by EXIT-based Link Adaptation Algorithm according to the instantaneous SNR of $R-D$ link, will be feedback to the encoder and modulator at the relay, then the code rate and modulation will be selected by the EXIT-based Link Adaptation Algorithm in Algorithm 4.1. In phase 2 slot 3, the relay will forward the information sequences. After decoding, we can obtain the reverted information sequence.

5.2 Theoretical Analysis

Firstly, we can divide all the situations into two cases according to using PLF system or not. As shown in Fig.5.2, in case 1, the information is only transmitted from source to destination due to the bad condition of the channel. The effective time consuming is T_{case1}. In case 2, the information is broadcast to the relay and destination in phase 1, and in phase 2, relay forwarded the information sequences to the destination. To simplify

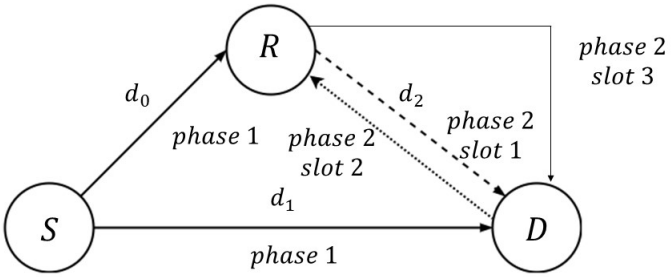

Figure 5.1: The system model for LALFOR system(cited from Fig.2.1)

calculation, we ignore the time of acquiring and feedback between relay and destination. Then the effective time consuming for case 2 is T_{case2}. Then the total effective time consuming can be expressed as

$$T_{total} = T_{case1} + T_{case2}, \tag{5.1}$$

We assume M for bits per symbol in the modulation method and R_c for the code rate. Since the modulation method and code rate for $S-D$ link and $S-R$ link remain QPSK and 1/2, the $M_{sd} = M_{sr} = 2$ and $R_{c,sd} = R_{c,sr} = 1/2$. The T_{case1} can be expressed as:

$$T_{case1} = (\frac{1}{M_{sd}R_{c,sd}}) \times p(success|case1) \times p(case1) \tag{5.2}$$

where p(success—case 1) denotes the probability of successful transmission in case 1, which can be expressed as $(1 - FER_{case1})$ and p(case 1) denotes the probability of case 1 happens, which can be expressed as energy efficiency η_{th}, as defined in (3.14).
Similarly, the T_{case2} can be expressed as

$$T_{case2} = \big(\frac{1}{M_{sr}R_{c,sr}} \times 1 + \frac{\sum_{j=1}^{L}\sum_{i=1}^{L}\frac{1}{M_jR_{c,i}}p(M_jR_{c,i}|success)}{N}\big) \times p(case2) \tag{5.3}$$

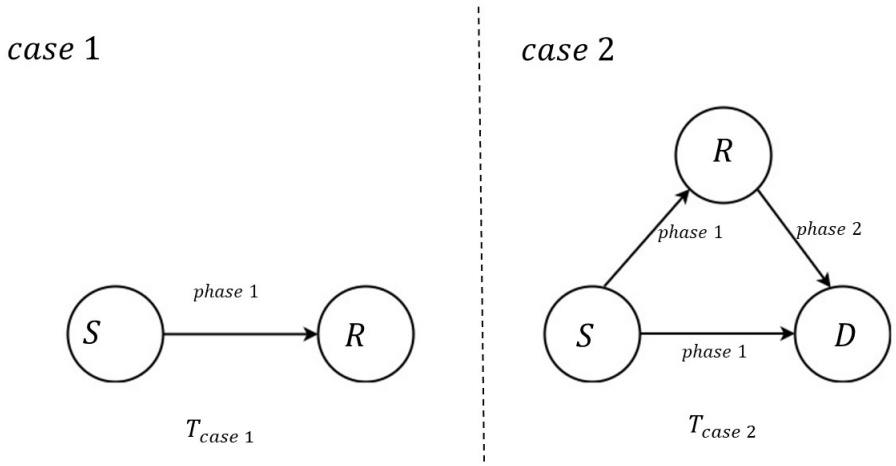

Figure 5.2: The different cases in LALFOR system

where L denotes the set of the modulation method and code rate according to the EXIT-based Link Adaptation Algorithm, N denote the total number of the frames, p(case 2) denotes the probability that case 2 happens, which can be expressed as (1-η_{th}). The $p(M_jR_{c,i}|success)$ denotes in the case of successful transmission, the probability for set $M_jR_{c,i}$ happens, which can obtain from the Bayes' theorem:

$$p(M_j, R_{c,i}|success) = p(success|M_jR_{c,i}) \times \frac{p(M_j, R_{c,i})}{p(success)} \tag{5.4}$$

with $p(success|M_jR_{c,i})$ denoting if the set $M_jR_{c,i}$ is being selected, the probability of successful transmission, expressed as $(1 - FER_{M_jR_{c,i}})$ in the simulation results. Also, $p(M_j, R_{c,i})$ express the probability of selecting this set, which can be directly calculated from the simulation and $p(success)$ denotes the probability of successful transmission over all case 2, expressed as $1 - FER_{case2}$. Also, for verification, we calculated $p(failure|M_jR_{c,i})$ as:

$$p(M_j, R_{c,i}|failure) = p(failure|M_jR_{c,i}) \times \frac{p(M_j, R_{c,i})}{p(failure)} \tag{5.5}$$

where $p(failure|M_jR_{c,i})$ is probability of unsuccessful transmission and $p(failure)$ is the total unsuccessful transmission in case 2.
From (5.4) and (5.5), we verified $\sum_{j=1}^{L}\sum_{i=1}^{L} p(M_jR_{c,i}|success) = 1$ and $\sum_{j=1}^{L}\sum_{i=1}^{L} p(M_jR_{c,i}|failure) = 1$.

Then, we define throughput efficiency improvement as the consuming time ratio of the case we want to compare with to the LALFOR case.

$$E = \frac{T_{total,the\,other\,case}}{T_{total,LALFOR\,case}} \tag{5.6}$$

5.3 Numerical Results

As shown in Fig.5.3, we firstly compared the case using LALFOR system with the case only using EXIT-based Link Adaptation Algorithm. Then, the throughput efficiency improvement E is defined as $E = \frac{T_{total,only\,LA}}{T_{total,LALFOR}}$. From the figure, we can clearly see that in the low SNR area, we can achieve higher improvement of throughput efficiency. That is because in the low SNR area, more frames will be transmitted from point to point channel, then more time will be save from only 1 phase transmission. Then we compared the case using LALFOR system with the case only using thresholding. Then, the throughput efficiency improvement E is defined as $E = \frac{T_{total,only\,Thresholding}}{T_{total,LALFOR}}$ We can also find the improvement in the high SNR area due to the time saving from the LA algorithm. After that, we compared the case using LALFOR system with the case using traditional Lossy-Forwaridng system only, which means LA and thresholding are not used in this case. The throughput efficiency improvement E is defined as $E = \frac{T_{total,LF\,system}}{T_{total,LALFOR}}$. We can find out that the improvement is increasing in both high and low SNR area, which means the LALFOR system can improvement throughput efficiency whatever the channel condition is. Also, we can see the energy efficiency in theoretical and practical results in Fig.5.4. There exist about 8% gap between theoretical and practical results and up to 50% energy can be saved when setting γ_{th}=1dB

5.4 Summary

In this chapter, firstly, we explain the principle of the LALFOR system and define the time consuming T for different cases, the throughput efficiency improvement E. Then, we obtain the throughput efficiency improvement E in different cases and calculate the energy efficiency η_{th} in LALFOR system. Finally, we draw the conclusion that, within LALFOR system, the throughput efficiency for the whole system can be improved whatever channel condition is.

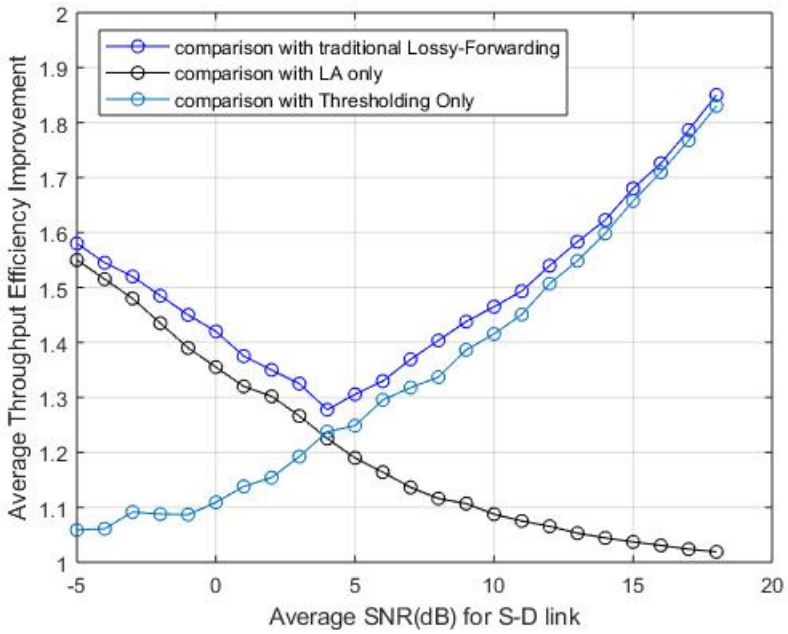

Figure 5.3: Throughput Efficiency Improvement in different cases

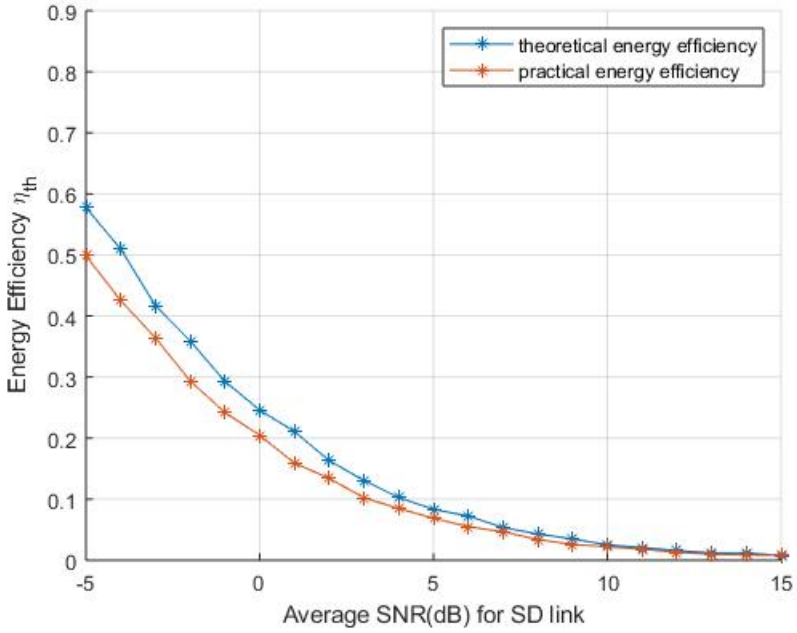

Figure 5.4: Energy Efficiency for LALFOR system when setting γ_{th}=1dB

Chapter 6

Conclusion

6.1 Conclusion

This thesis has investigated two important issues, which are energy efficiency and throughout efficiency according to the channel condition in the single-relay system; the lower energy consumption and the shorter time consumption are better. To achieve the two objecives, the results have been obtained as following:
In Chapter 2, first of all, we described the principle of Lossy forwarding system has been introduced. Then, the fundamental knowledge of BICM-ID and joint-decoding scheme was proposed as the research background.
In Chapter 3, then, the system model of PLF System was introduced. After that, from the Shannon's lossy source-channel separation theorem and the theorem for source coding with side information, we obtained the exact outage probability. Then, by using numerical integration, the theoretical analysis for PLF system was implemented. We found that by using PLF system, we can save energy in spite of increase of outage probability and decrease of communication coverage. We run chain-simulation for PLF system over fading channel. We verified simulation results are consistent to the theoretical results. Then, to compensate the geometric loss caused by channel model, we introduced the vertical distance V_D from the relay to the destination. We found that if the larger energy efficiency improvement can be achieved, the greater vertical distance V_D is, although outage probability also increase.
In Chapter 4, we introduced the principle of EXIT analysis. Then, the Constellation Constrained Capacity was introduced as a tool for EXIT-based Link Adaptation Algorithm. After that, we introduced the principle and procedure of EXIT-based Link Adaptation Algorithm. By theoretical analysis followed by chain simulation, we found that the outage probability of the EXIT-based Link Adaptation Algorithm is between only using the lowest code rate and modulation set and only using the highest code rate and modulation set.

In Chapter 5, we introduced the LALFOR system model initially, then clarified the definition of time consuming and throughput efficiency improvement. As a conclusion, we found that the LALFOR system could improve throughput efficiency whatever channel condition is.

6.2 Future Work

Based on the results achieved by this thesis, we can provide several directions as the future work.

- We can further expand the set of the code rate and modulation method to increase the suitability of the EXIT-based Link Adaptation Algorithm to increase the applicability of the algorithm.
- We can apply LALFOR system to the multiple relay system with the scope of further generalization of the LALFOR concept.

Appendix A

Exact Outage Probability Calculation for traditional Lossy-Forwarding System

From [7], we can know that the outage probability is divided into four parts as:

$$\begin{aligned} P_{out}^{'} &= \Pr(0 \le p \le 0.5, (R_1, R_2)\epsilon(R_A \cup R_B)) \\ &= \Pr(p = 0, (R_1, R_2)\epsilon R_A) \\ &+ \Pr(p = 0, (R_1, R_2)\epsilon R_B) \\ &+ \Pr(0 < p \le 0.5, (R_1, R_2)\epsilon R_A) \\ &+ \Pr(0 < p \le 0.5, (R_1, R_2)\epsilon R_B). \end{aligned} \tag{A.1}$$

Then, let $P_{1,a}^{'} = \Pr(p = 0, (R_1, R_2)\epsilon R_A)$,$P_{1,b}^{'} = \Pr(p = 0, (R_1, R_2)\epsilon R_B)$,$P_{2,a}^{'} = \Pr(0 < p \le 0.5, (R_1, R_2)\epsilon R_A)$,$P_{2,b}^{'} = \Pr(0 < p \le 0.5, (R_1, R_2)\epsilon R_B)$. Then $P_{1,a}^{'}$, $P_{1,b}^{'}$, $P_{2,a}^{'}$,$P_{2,b}^{'}$ are expressed as:

$$\begin{aligned} P_{1,a}^{'} &= Pr\left\{p = 0, R_2 \ge 1, 0 \le R_1 \le H_b(p)\right\} \\ &= Pr\left\{\gamma_0 \ge \Phi_1^{-1}(1), \gamma_2 \ge \Phi_2^{-1}(1), \Phi_1^{-1}(0) \le \gamma_1 \le \Phi_1^{-1}(0)\right\} \\ &= \int_{\Phi_1^{-1}(0)}^{\Phi_1^{-1}(1)} d\gamma_0 \int_{\Phi_2^{-1}(0)}^{\Phi_2^{-1}(1)} d\gamma_2 \int_{\Phi_1^{-1}(0)}^{\Phi_1^{-1}(1)} p(\gamma_0) \cdot p(\gamma_1) \cdot p(\gamma_2) d\gamma_1 \\ &= 0 \end{aligned} \tag{A.2}$$

$$\begin{aligned} P_{1,b}^{'} &= Pr\left\{p = 0, 0 \le R_2 \le 1, 0 \le R_1 \le H_b(\alpha * p)\right\} \\ &= Pr\left\{\gamma_0 \ge \Phi_1^{-1}(1), \Phi_2^{-1}(0) \le \gamma_2 \le \Phi_2^{-1}(1), \Phi_1^{-1}(0) \le \gamma_1 \le [1 - \Phi_2(\gamma_2)]\right\} \\ &= \int_{\Phi_1^{-1}(0)}^{\Phi_1^{-1}(\infty)} d\gamma_0 \int_{\Phi_2^{-1}(0)}^{\Phi_2^{-1}(1)} d\gamma_2 \int_{\Phi_1^{-1}(0)}^{\Phi_1^{-1}[1-\Phi_2(\gamma_2)]} p(\gamma_0) \cdot p(\gamma_1) \cdot p(\gamma_2) d\gamma_1 \\ &= \frac{1}{\Gamma_2} \exp\left[-\frac{\Phi_1^{-1}(1)}{\Gamma_0}\right] \int_{\Phi_2^{-1}(0)}^{\Phi_2^{-1}(1)} \exp(-\frac{\gamma_2}{\Gamma_2}) \cdot \left[1 - \exp(-\frac{\Phi_1^{-1}\left[1 - \Phi_2(\gamma_2)\right]}{\Gamma_1})\right] d\gamma_2 \end{aligned} \tag{A.3}$$

$$
\begin{aligned}
P_{2,a}^{'} &= Pr\left\{0 < p \leq 0.5, 0 \leq R_2 \leq 1, 0 \leq R_1 \leq H_b(p)\right\} \\
&= Pr\left\{\Phi_1^{-1}(0) \leq \gamma_0 \leq \Phi_1^{-1}(1), \gamma_2 \geq \Phi_2^{-1}(1), \Phi_1^{-1}(0) \leq \gamma_1 \leq [1-\Phi_1(\gamma_0)]\right\} \\
&= \int_{\Phi_1^{-1}(0)}^{\Phi_1^{-1}(1)} d\gamma_0 \int_{\Phi_2^{-1}(0)}^{\Phi_2^{-1}(\infty)} d\gamma_2 \int_{\Phi_1^{-1}(0)}^{\Phi_1^{-1}[1-\Phi_1(\gamma_0)]} p(\gamma_0)\cdot p(\gamma_1)\cdot p(\gamma_2) d\gamma_1 \\
&= \frac{1}{\Gamma_0}\exp\left[-\frac{\Phi_2^{-1}(1)}{\Gamma_2}\right] \int_{\Phi_2^{-1}(0)}^{\Phi_2^{-1}(1)} \exp(-\frac{\gamma_0}{\Gamma_0})\cdot\left[1-\exp(-\frac{\Phi_1^{-1}\left[1-\Phi_1(\gamma_0)\right]}{\Gamma_1})\right] d\gamma_0
\end{aligned}
\tag{A.4}
$$

$$
\begin{aligned}
P_{2,b}^{'} &= Pr\left\{0 < p \leq 0.5, 0 \leq R_2 \leq 1, 0 \leq R_1 \leq H_b(\alpha * p)\right\} \\
&= Pr\left\{\Phi_1^{-1}(0) \leq \gamma_0 \leq \Phi_1^{-1}(1), \gamma_2 \geq \Phi_2^{-1}(1), \Phi_1^{-1}(0) \leq \gamma_1 \leq \Phi_1^{-1}\left[\Psi(\gamma_0,\gamma_2)\right]\right\} \\
&= \int_{\Phi_1^{-1}(0)}^{\Phi_1^{-1}(1)} d\gamma_0 \int_{\Phi_2^{-1}(0)}^{\Phi_2^{-1}(\infty)} d\gamma_2 \int_{\Phi_1^{-1}(0)}^{\Phi_1^{-1}[\Psi(\gamma_0,\gamma_2)]} p(\gamma_0)\cdot p(\gamma_1)\cdot p(\gamma_2) d\gamma_1 \\
&= \frac{1}{\Gamma_0\Gamma_2} \int_{\Phi_1^{-1}(0)}^{\Phi_1^{-1}(1)} \int_{\Phi_2^{-1}(0)}^{\Phi_2^{-1}(1)} \exp(-\frac{\gamma_0}{\Gamma_0}-\frac{\gamma_2}{\Gamma_2})\cdot\left[1-\exp(-\frac{\Phi_1^{-1}\left[\Psi(\gamma_0,\gamma_2)\right]}{\Gamma_1})\right] d\gamma_0 d\gamma_2.
\end{aligned}
\tag{A.5}
$$

Since it is difficult to derive the explicit expressions of those integration, we calculate them by numerical technique

References

[1] A. K. Sadek, W. Su, and K. J. R. Liu, "Multinode cooperative communications in wireless networks," *IEEE Transactions on Signal Processing*, vol. 55, no. 1, pp. 341–355, 2007.

[2] Y. Li, "Distributed coding for cooperative wireless networks: An overview and recent advances," *IEEE Communications Magazine*, vol. 47, no. 8, pp. 71–77, 2009.

[3] J. He, V. Tervo, X. Zhou, X. He, S. Qian, M. Cheng, M. Juntti, and T. Matsumoto, "A tutorial on lossy forwarding cooperative relaying," *IEEE Communications Surveys Tutorials*, vol. 21, no. 1, pp. 66–87, 2019.

[4] M. Cheng, K. Anwar, and T. Matsumoto, "On the duality of source and channel correlations: Slepian-wolf relaying viewpoint," in *2012 IEEE International Conference on Communication Systems (ICCS)*, 2012, pp. 388–392.

[5] K. Anwar and T. Matsumoto, "Accumulator-assisted distributed turbo codes for relay systems exploiting source-relay correlation," *IEEE Communications Letters*, vol. 16, no. 7, pp. 1114–1117, 2012.

[6] M. Cheng, A. Irawan, K. Anwar, and T. Matsumoto, "Bicm-id for relay system allowing intra-link errors and a similarity constellation to arq schemes," *Progress In Electromagnetics Research Symposium (PIERS)*, 01 2012.

[7] X. Zhou, M. Cheng, X. He, and T. Matsumoto, "Exact and approximated outage probability analyses for decode-and-forward relaying system allowing intra-link errors," *IEEE Transactions on Wireless Communications*, vol. 13, no. 12, pp. 7062–7071, 2014.

[8] S. Qian, M. Cheng, and T. Matsumoto, "Outage based power allocation for a lossy-forwarding relaying system," 06 2015.

[9] W. Lin, S. Qian, and T. Matsumoto, "Lossy-forward relaying for lossy communications: Rate-distortion and outage probability analyses," *IEEE Transactions on Wireless Communications*, vol. 18, no. 8, pp. 3974–3986, 2019.

[10] K. W. Cattermole, "History of pulse code modulation," *Proceedings of the Institution of Electrical Engineers*, vol. 126, no. 9, pp. 889–892, 1979.

[11] R. Youssef and A. G. i. Amat, "Distributed serially concatenated codes for multi-source cooperative relay networks," *IEEE Transactions on Wireless Communications*, vol. 10, no. 1, pp. 253–263, 2011.

[12] W. M.Schwartz and S.Stein, *Communications systems and techniques*. WILEY: IEEE Commun.Mag, 1996.

[13] S. Pfletschinger and F. Sanzi, "Error floor removal for bit-interleaved coded modulation with iterative detection," *IEEE Transactions on Wireless Communications*, vol. 5, no. 11, pp. 3174–3181, 2006.

[14] E. Zehavi, "8-psk trellis codes for a rayleigh channel," *IEEE Transactions on Communications*, vol. 40, no. 5, pp. 873–884, 1992.

[15] A. Chindapol and J. A. Ritcey, "Design, analysis, and performance evaluation for bicm-id with square qam constellations in rayleigh fading channels," *IEEE Journal on Selected Areas in Communications*, vol. 19, no. 5, pp. 944–957, 2001.

[16] B. L.Hanzo, T.H.Liew, *Turbo coding,Turbo Equalisation and Space-Time Coding for Transmission over fading Channels*. Cambridge, UK: John Wiley Sons,LTD, 2002.

[17] Xiaodong Li and J. A. Ritcey, "Bit-interleaved coded modulation with iterative decoding," in *1999 IEEE International Conference on Communications (Cat. No. 99CH36311)*, vol. 2, 1997, pp. 858–863 vol.2.

[18] K. Anwar and T. Matsumoto, "Very simple bicm-id using repetition code and extended mapping with doped accumulator," *Wireless Personal Communications*, vol. 67, no. 3, pp. 573–584, Dec 2012.

[19] J. Garcia-Frias and Ying Zhao, "Near-shannon/slepian-wolf performance for unknown correlated sources over awgn channels," *IEEE Transactions on Communications*, vol. 53, no. 4, pp. 555–559, 2005.

[20] S. ten Brink, "Convergence behavior of iteratively decoded parallel concatenated codes," *IEEE Transactions on Communications*, vol. 49, no. 10, pp. 1727–1737, 2001.

[21] F. Brannstrom, L. K. Rasmussen, and A. J. Grant, "Convergence analysis and optimal scheduling for multiple concatenated codes," *IEEE Transactions on Information Theory*, vol. 51, no. 9, pp. 3354–3364, 2005.

[22] J. Hagenauer, "The exit chart - introduction to extrinsic information transfer in iterative processing," in *2004 12th European Signal Processing Conference*, 2004, pp. 1541–1548.

[23] Feng Yunfei and Li Jianping, "Optimized symbol mapping for bit-interleaved coded modulation with iterative decoding," in *2008 11th IEEE International Conference on Communication Technology*, 2008, pp. 237–240.

[24] Axel Dauch, "Frequency domain turbo equalization with extended mapping," in *Master Thesis of JAIST*, 2007.

[25] G. Ungerboeck, "Channel coding with multilevel/phase signals," *IEEE Transactions on Information Theory*, vol. 28, no. 1, pp. 55–67, 1982.

[26] Nishioka Kenichi, "Theoretical analyses of constellation constrained capacity and their verification using field measurement data," in *Master Thesis of JAIST*, 2010.

[27] Y. D. Li Weidong, Yang Hongwen, "Approximation formulas for the symmetric capacity of m-ary modulation," *Science paper online*, vol. 42, no. 8, pp. 3254–3164, 2010.

[28] S. Ibi, T. Matsumoto, R. ThomÄThoma, S. Sampei, and N. Morinaga, "Exit chart-aided adaptive coding for multilevel bicm with turbo equalization in frequency-selective mimo channels," *IEEE Transactions on Vehicular Technology*, vol. 56, no. 6, pp. 3757–3769, 2007.